Bachelor Thesis

Optimization of Polyelectrolyte Multilayer Capsules

Optimierung der Polyelektrolyt Kapseln

by

Gertrud S. D. Stalmann

Submitted to Prof. Dr. Wolfgang J. Parak
Second assessor Prof. Dr. Kerstin Volz
Supervised by Carolin Ganas, Markus Ochs
Department Biophotonics / Faculty of physics

Philipps–Universität Marburg

July 3, 2010

Contents

Abstract

Polyelectrolyte multilayer capsules based on $CaCO_3$ and SiO_2 cores coated with the polyelectrolyte systems PAH/PSS and PDADMAC/PSS have been analyzed. A series of measurement has been conducted to study the impact of temperature, rotation speed during precipitation and concentration of the stock solutions on the $CaCO_3$ core diameter. Also the effect of annealing on the empty capsules has been observed. As a result an impact of the heating on the diameter was observed, but in a few cases swelling was detected although shrinking was expected. Furthermore a strong dependency of the $CaCO_3$ particle size on the rotation speed during the particle precipitation has been observed. The $CaCO_3$ microspheres increased in size if the rotation speed was decreased from 1200 rpm to 250 rpm while in general keeping their monodisperse character. This could be used to obtain monodisperse particles with tunable size that can be employed in a wide field of applications like biotechnology, medicine or catalysis.

Polyelectrolyt Multilayer Kapseln aus PAH/PSS und PDADMAC/PSS wurden auf Basis von $CaCO_3$ und SiO_2 hergestellt. Ihre Größe wurde einerseits durch Änderung des Templatdurchmessers und andererseits durch thermische Behandlung der leeren Polyelectrolytkapseln variiert.
Bei dem Erhitzen der Kapseln wurde eine Änderung des Durchmessers beobachtet, allerdings kam es nur bei einem Teil der Kapseln zu der erwarteten Verkleinerung. Sobald diese Methode zuverlässig funktioniert, könnten so Moleküle mit geringem Molekulargewicht, nach Diffusion durch die Polyelektrolythülle, sicher in den Hohlraum der Kapseln eingeschlossen werden.
Um den Templatdurchmesser zu beeinflussen wurde der Einfluss dreier Parameter auf die Partikelgröße untersucht. Diese Parameter waren Rührgeschwindigkeit während der Synthese, Temperatur der Ausgangslösungen und Konzentration der Lösungen während der Reaktion.
Hierbei wurde für die Rührgeschwindigkeit der Zusammenhang entdeckt, dass die Partikel bei einer Reduzierung der Rührgeschwindigkeit von 1200 rpm auf 250 rpm größer wurden. Mit der Partikelvergrößerung ging bei diesem Parameter zusätzlich keine starke Verbreiterung der Größenverteilung einher. Deshalb sind Polyelektrolytkapseln auf Basis solcher monodisperser und biokompatibler Mikropartikel mit einer beeinflussbaren Größe gut geeignet für Anwendungen wie zum Beispiel Biotechnologie, Medizin und Chemie.

1 Introduction

In the 1990's the method of layer–by–layer thin films was developed by Decher et al. [1] on flat surfaces. It is based on the electrostatic attraction of oppositely charged functional groups, that can subsequently be adsorbed onto a charged template. The driving force of this method is charge overcompensation after each layer [2] which allows several layers to be applied.

In particular polyelectrolytes as layer material have several advantages: Because of their ionic nature polyelectrolytes can be adsorbed from aqueous solution in a cheap and environmentally friendly way. Moreover the coating with polyelectrolytes is mostly independent of the template form as long as it has a surface charge. Soon the potential to coat also spherical particles was found out as well as the fact, that after core removal spherical hollow capsules are obtained. These capsules can be loaded with molecules of different molecular weight and the polyelectrolyte walls can be functionalized additionally with nanoparticles[3]. The production of these polyelectrolyte multilayer capsules is of great interest because of their potential as drug delivery systems[11] with controlled releasing properties[12][16][3], as sensor systems [26], as microreactors[13][14][15], as catalytic systems[13][14], etc.
The basic polyelectrolyte multilayer capsule is composed of two components: the sacrificial core and the polyelectrolyte multilayer wall. The coating process for the typical system $(PSS/PAH)_n$ on $CaCO_3$ can be seen in figure 1.

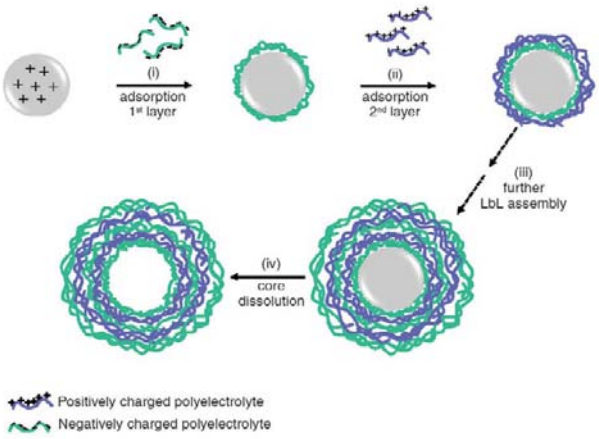

Fig. 1: Fabrication of hollow polyelectrolyte microcapsules via layer-by-layer assembly, taken from reference [3]

1.1 Templates

For the template a wide range of materials have been used. If the spherical particle is not the cargo itself, these templates are sacrificial. This is the case most of the time. Generally, polyelectrolyte capsules are permeable to small molecules with a dimension of a few nanometers, but impermeable to bigger molecules. Thus the core can be removed, if the particles fulfill the qualification of being dividable into low molecular weight fragments.
Materials used until now reach for example from organic colloids like polystyrene latex [4] and melamine formaldehyde (MF)[10] to inorganic template materials like $CaCO_3$[9] to SiO_2[16].
They differ significantly in their properties like monodispersity, porosity and solubility as well as biocompartibility.
While $CaCO_3$ cores can be dissolved easily and environmentally friendly with aqueous ethylenediaminetetraacetic acid (EDTA) solution, their size range is relatively large and difficult to control. SiO_2 cores on the other hand can be produced monodispersely but their solution with HF is complicated because of its low dissociation constant. The originally employed weakly crosslinked MF particles dissolve at low pH, but some MF oligomers can remain[10]. Because of the biological incompatibility these cores are limited in their use and not further analyzed in this work.
A further property that depends on the core is the loading method. In general the methods are categorized in 'pre–loading' and 'post–loading' methods.
If 'pre–loading' is used either the cores are filled by coprecipitation with the molecules before the layer–by–layer assembly or the molecules are adsorbed onto the porous core surface before coating.
In the 'post–loading' strategy hollow capsules are produced that are loaded afterwards by changing the permeability of the capsule walls. This can be achieved for example by changing the pH or the temperature and can be reversible or irreversible.
In the presented work the pre–loading method is used with $CaCO_3$ particles and for SiO_2 cores post–loading is used.

$CaCO_3$ Cores

$CaCO_3$ particles show many of the desired properties for templates and have therefore been studied a lot recently. For the composition of $CaCO_3$ different reactions can be used. In this work $NaCO_3$ and $CaCl_2$ have been used so that, following the reaction equation 1, calcium carbonate is produced.

$$CaCl_2 + Na_2CO_3 \rightarrow 2NaCl + CaCO_3 \quad (1)$$

There are several polymorphs in which $CaCO_3$ can crystallize:
Calcite is the thermodynamically most stable form of $CaCO_3$ and is widely available in nature. Its crystal structure is trigonal-rhombohedral and consists of alternate CO_3^{2-} and Ca^{2+} layers.
Aragonite is thermodynamically less stable but often found in nature. Alternating CO_3^{2-} and Ca^{2+} layers are arranged in an orthorhombic crystal structure.
Vaterite is a thermodynamical metastable form rarely found in nature. It has an hexagonal crystal structure of alternating CO_3^{2-} and Ca^{2+} layers.
For the usage as sacrificial cores for polyelectrolyte multilayer capsules spherical charged particles with a size of 2 μm-8 μm are needed. For this purpose the polymorph vaterite is applicable, since the small vaterite crystals ($\approx 50nm$) aggregate to spherical particles of the desired size range[17] and surface potential[19].
Amorphous $CaCO_3$, that does not have a long range order of the atom position, also forms particles in the desired size range[21]. These particles are in general spherical and obtain a vaterite coating after 30 min[18], so that they could be used as template for polyelectrolyte adsorption. In this work no structure analysis has been done, so it could not be distinguished whether clusters of vaterite or amorphous $CaCO_3$ was the final product in the reaction. Nonetheless mainly vaterite particles are expected, because Yan et al. reported, that the crystallization of $CaCO_3$ particles depends on the stirring speed during precipitation. By X-ray diffraction they found out, that the spherical particles consisted mainly of vaterite while the hexahedral crystals were mainly composed of calcite[20].
In figure 2 A-C SEM pictures of the resulting particles are shown. In order to coat these particles it is important to know the polarity of their charge. Volodkin et al.[5] found out, that the surface charge of $CaCO_3$ particles depends on the pH of the surrounding fluid. For pH 7 and 8 the surface charge is positive and for pH 9 and 10 the zeta–potential changes to negative. The $CaCO_3$ particles produced this way are reported to be porous and to have a rather big surface area[7]. Because of this they are particularly suitable for pre–loading via coprecipitation.
Because neither the vaterite nor the amorphous $CaCO_3$ is stable, it is necessary to either dry the spheres for storage or to coat them in order to prevent the formation of the more stable calcite or aragonite.
After the assembly of the desired number of polyelectrolyte layers the $CaCO_3$ core can be removed from the microsphere using EDTA as the chelating agent under mild conditions. This procedure has been reported to not affect the encapsulated material[9].

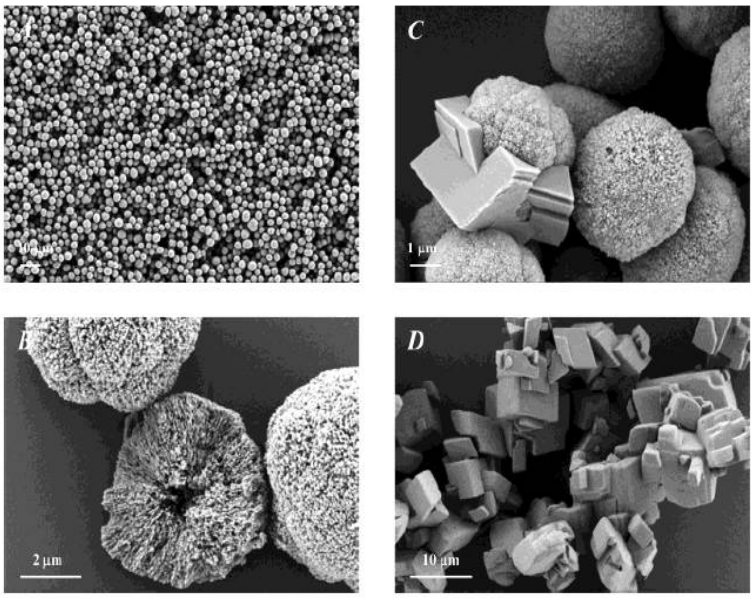

Fig. 2: SEM images of $CaCO_3$ particles. A, in Overview; B, broken particle; C, recrystallization of a particle; D, calcium carbonate microcrystals from Aldrich, taken from reference [5]

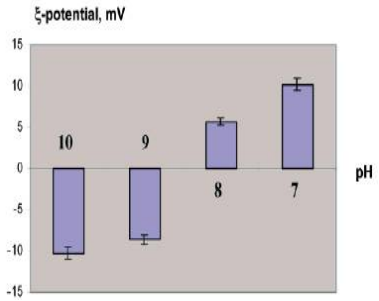

Fig. 3: Change of ζ–potential in mV of $CaCO_3$ microparticles as a function of pH, taken from reference [5]

SiO_2 cores

For the preparation of hollow microcapsules based on SiO_2 as template, a commercial product was used (4.78+/-0.19 μm).
In order to dissolve the cores after coating 0.3 M hydrofluoric acid is used following the reaction 2.

$$SiO_2 + 4HF \rightarrow SiF_4 + 2H_2O \tag{2}$$

This procedure is more hazardous because of the acid and therefore needs to be handled with special care. However the monodisperse and non aggregated SiO_2 microsheres are apt for polyelectrolyte capsule preparation.

1.2 Polyelectrolyte capsule walls

The capsule walls are build by polycation–polyanion complexes that are formed through electrostatic interaction. In order to understand this mechanism it is necessary to have a closer look at polyelectrolytes.
Polyelectrolytes are charged polymers in which each monomer has at least one functional group that can be charged. They are divided into 'strong' and 'weak' polyelectrolytes describing their charge dependency on the pH. Strong polyelectrolytes have a charge that is mainly independent of pH while for weak polyelectrolytes the charge can be modified by changing the pH. An attribute with that they can be categorized is their acid dissociation constant K_a that is the equilibrium constant for the dissociation:

$$HA \rightleftharpoons A^- + H^+ \tag{3}$$

The dissociation constant can then be written as the quotient of the A^-, H^+ and HA equilibrium concentrations:

$$K_a = \frac{[A^-][H^+]}{[HA]} \tag{4}$$

In order to reduce the range of this constant the negative decadic logarithm is often used:

$$pK_a = -log_{10}K_a \tag{5}$$

Polyelectrolytes with a small pK_a value are considered strong. In contrast they have the characteristics of weak polyelectrolytes, if the pK_a value is between ≈ 2 and ≈ 10.
The amount of charged functional groups has also an effect on the structure of the polyelectrolyte: The more functional groups are charged the more the polyelectrolyte is stretched because of electrostatic repulsion. Therefore a less charged weak polyelectrolyte will have a rather coiled polymer conformation.

The system PSS/PAH

Poly(allylamine) (PAH) and Poly(styrenesulfonate) (PSS) are polyelectrolytes whose properties in multilayer build up are well studied. PSS is a strong polyanion with a pK_a value of about 2 while PAH has a pK_a value of about 8.5 and therefore is a weak polycation. In order to have a system in which a similar amount of both polyelectrolytes is adsorbed, nearly equally charged polymers are necessary. Because of that PAH with a pH of 6.5 is typically used for the coating.
It has been shown, that capsules build of $(PSS/PAH)_n$ multilayers change their size if heated. This effect will be explained further later.

The system PSS/PDADMAC

Poly(diallyldimethylammoniumchlorid) (PDADMAC) is like PSS a strong polyelectrolyte and has an cationic character. Earlier studies have shown, that hollow capsules with an even polyelectrolyte number and PSS as the outmost layer shrink upon temperature increase. The wall thickness increases during this process and consequently the permeability for smaller molecules should decrease[25].
The structure of PSS, PAH and PDADMAC is displayed in figure 4.

1.3 Heat sensitivity

The procedure of post–loading is especially interesting for macromolecules with particularly high or low molecular weight.
For the system PDADMAC/PSS it has been observed, that a swelling of the capsule resulted in a decrease of wall thickness while the wall thickness increased during capsule shrinking[23].

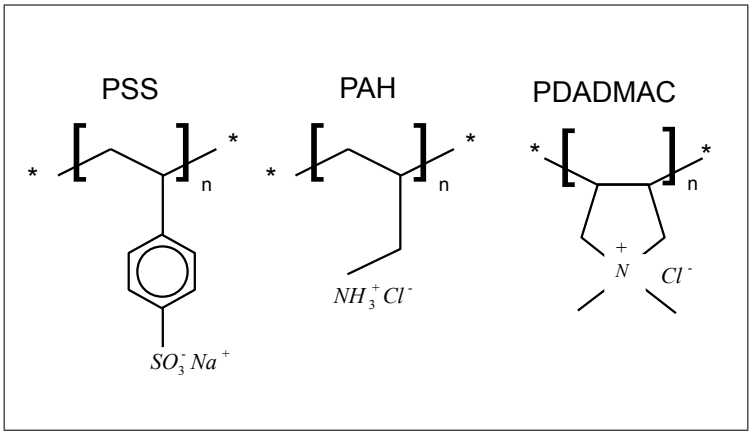

Fig. 4: Chemical structure of PSS, PAH and PDADMAC

This suggests, that the permeability increases with swelling and decreases during shrinking. In order to use this effect for amplification of the loading possibility, the thermal behavior of polyelectrolyte capsules has been under examination.
Two systems, that are sensitive to the temperature have been described above: The systems PAH/PSS and PDADMAC/PSS.
The change in size seems to be dependent on the system used, the number of layers[24] and the charge of the last layer. The results for even layer number given in the literature are summarized in the table below.

Polyelectrolyte	**Last layer**	**Thermal effect**
PSS/PDADMAC	PDADMAC	swelling (reversible)[23]
PDADMAC/PSS	PSS	shrinking (irreversible)[25]
PSS/PAH	PAH	shrinking (irreversible)[27][31]
PAH/PSS	PSS	shrinking (irreversible)

Table 1: Thermal effect on polyelectrolyte multilayer capsules

Additionally it has been shown, that corresponding with the (PDADMAC/PSS) capsule shrinking the wall thickness increased and the permeability for low molecular weight macromolecules is decreased[28]. These properties allow to post–load hollow capsules with (PDADMAC/PSS) walls via heat shrinking and to encapsulate molecules with a low molecular weight (10 kDa)[29]. The swelling of capsules with PDADMAC as the last layer was explained with an electrostatic repulsion of the excess positive charge[23], while the shrinking in the case of PSS as last layer

was explained with a polymer rearrangement to reduce the surface tension [25]. The procedure applied in this work was mainly according to W.Song et al.[30].

1.4 Goal

As explained above the fabrication of polyelectrolyte multilayer capsules based on $CaCO_3$ cores is of great interest. For this production it is necessary to be able to influence the particle size and to get as high reproducibility as possible. With capsules based on size controlled and monodisperse particles, the opening of with gold nanoparticles functionalysed capsules can be analyzed better and the usage as sensor system can be improved. Because the precipitation process of $CaCO_3$ is influenced by several aspects, the aim of this work is to optimize the influencability of size.
Once the problem of the size range is solved, finding a way to load the capsules with particles of low molecular weight is desirable. In order to accomplish this, it would be necessary to reduce the permeability of capsules. The idea is to archive the permeability reduction by using heat sensitive polyelectrolytes that show an irreversible size reduction at high temperatures. This 'heat shrinking' could be used to post–load capsules with low molecular weight molecules.

2 Analysis

For the analysis of the cores confocal laser scanning microscopy (LSM) was the main tool. The capsules were also analyzed by the LSM and the loading success was observed by fluorescence microscopy. In all experiments the macroscopical precipitation process has been observed as well as the dissolution process of the cores.

2.1 Confocal laser scanning microscopy

The basic idea of confocal laser microscopy is to focus on one point in the probe at a time and to ignore the rest of the reflected light. This way the sample can be scanned point by point and the resulting picture is a 2D cut of the area of interest. Thus a much higher resolution than with conventional microscopes can be achieved. By combining several 2D layers, a 3D picture of the sample can be produced and recorded.
A scheme how this idea is technically realized is shown in figure 5.

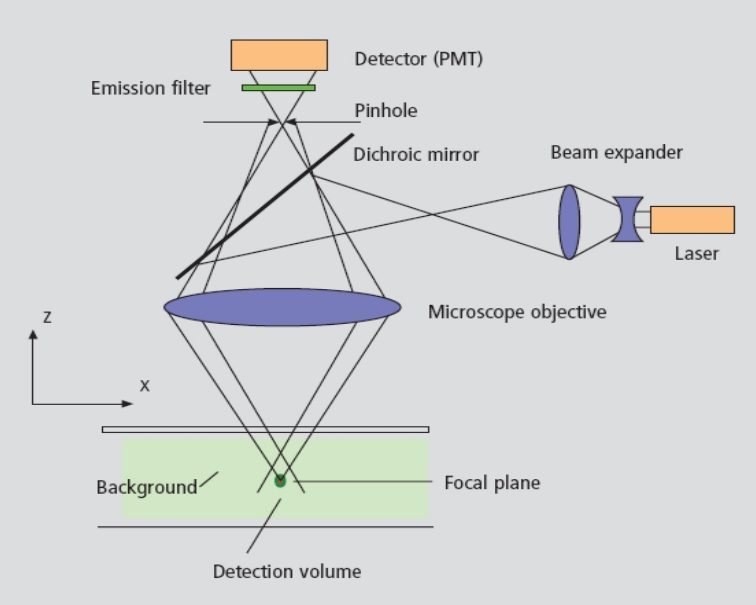

Fig. 5: Schematic structure of a confocal laser scanning microscope, taken from reference [8]

The Laser beam is first expanded and directed to a dichroic mirror, that reflects only the part of the light with the selected wavelength. This light is focused by the objective and hits the sample. Fluorescent samples absorb the light and emit a light with a usually longer wavelength and lower energy. For non fluorescent probes the transmission channel is used in which the wavelength does not change. The emitted light with an apt wavelength passes the dichroic mirror again. In front of the detector a pinhole blocks the light from outside the focus point and an emission filter again selects the light with the desired wavelength range. Afterwards the remaining light reaches the detector and can be recorded. Because only one point in the focus level is recorded by this procedure, it is necessary to scan the whole probe to get a full picture.

2.2 Data interpretation

Size study

For the $CaCO_3$ size analysis a photo was taken with the LSM using the Zeiss software ZEN 2007. According to the magnification a scale bar of 5 μm was added. This picture was then loaded in the public domain program ImageJ in which the scale was set apt to the scale bar. Afterwards the picture was made binary and the aggregated templates were erased. If necessary the colors were inverted, so that the cores were represented by black circles. As soon as only nearly spherical and non aggregated templates were left, the program ImageJ could calculate the black areas. This data could then be transferred into diameter information via the following equation.

$$d = 2 \cdot \sqrt{\frac{A}{\pi}} \tag{6}$$

In this equation d gives the diameter in μm and A is the area in μm^2. In the following discussion the word size is used as a a synonym for the particle diameter. A source of error in this analysis is, that the $CaCO_3$ particles are not perfectly spherical. Therefore the diameter calculation using equation 6 is not exact. This error can be reduced by statistical analysis of many microparticles as has been done for these experiments.
Another problem is that in LSM pictures the choice of focus has an impact on the apparent size of the particle. As is shown in figure 6, the impact of this error is proportional to width of the size range: Particles smaller than the average will

seem to be even smaller, because the scanning layer will be above their middle section and bigger particles will also appear smaller because of the lower scanning layer. Therefore pictures with a low variation in particle size will be more exact. This effect could be reduced by analyzing one microsphere at a time with with the most suitable focus level. On the other hand this is a very time consuming procedure which has not been done for this analysis.

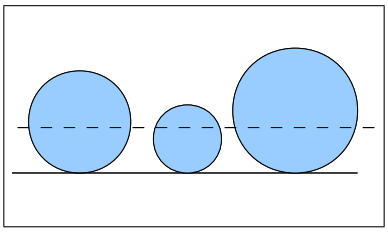

Fig. 6: The difficulty of focus for spheres with different sizes

Heat shrinking

The heat shrinking procedure consists of different steps, which are explained further in the section methods. In between the various steps the samples were looked at under the microscope. This way pictures were produced from before the coating, after the coating, after the core dissolution, after the incubation with the fluorescein isothiocyanate–Dextran (Dextran-FICT) and after the heat exposure. Additionally parts of the probes were dried after core dissolution in order to test, if the core was removed completely. The size distribution of SiO_2 based capsules was analyzed in the same way as for the $CaCO_3$ cores in order to evaluate the shrinking process. Furthermore the ability to load these capsules with fluorescent labeled 10 kDa Dextran was studied with a confocal fluorescence microscope as described above.

3 Experimental

Materials

milliQ water: deionized water (Millipore R$\geq$ 18.2$M\Omega$)was used for all solutions and washing steps
PAH (Poly(allylamin hydrochloride), Sigma, no. 283223, MW$\approx$ 56 000 g/mol): weak polycation
PDADMAC (Poly(diallyl dimethylammoniumchloride), Sigma, no. 409022 MW$\approx$ 350 000 g/mol)): strong polycation
PSS (Poly(sodium-4-styrolsulfonate), Aldrich, no. 243051, MW$\approx$ 70 000 g/mol): strong polyanion
EDTA (Ethylendiaminetetraacetic acid, Sigma, no. E5134): chelating agent for Ca^{2+} ions
HF (Hydrofluoric acid, 0,3M): dissolvent for silicon dioxide
SiO_2 spherical particles (diameter 4.78 $\pm$0.19 μm) template for capsules
Dextran Dextran (Mw 2000 kDa) and Dextran–FITC (fluorescein isothiocyanate–Dextran, Mw 10 kDa)
Na_2CO_3
$CaCl_2$

Equipment

Centrifuge Thermo Science,Varifuge 3.0RS for the $CaCO_3$ core dissolution and microfuge ALC, Centrifugette 4214 for the washing processes
Ultrasound sonicator Bandelin, Sonorex super RK103H
Magnetic stirrer
Vortex generator Sartorius, Certomat MO II
For analyzing the experiments always a Zeiss microscope with Argon Laser and a 100x Oil Immersion objective was used.

3.1 Methods

3.1.1 $CaCO_3$ core synthesis

For the $CaCO_3$ precipitation 0.3 M solutions of each $CaCl_2$ and Na_2CO_3 were prepared. As substituent for any cargo in the pre–loading method a solution of

Dextran 2000 kDa with the concentration $5\frac{mg}{ml}$ was prepared and mixed with the required amount $CaCl_2$ solution prior to precipitation with Na_2CO_3.
If not written otherwise the experiments were conducted at room temperature (20 °C-24.5 °C) in a lab environment (atmospheric pressure: 983 hPa-1020 hPa; humidity: 22 %-41.5 %). For each of the different test series one parameter was modulated as will be described afterwards.
In the beginning of the synthesis 770 μl of aqueous Dextran solution was mixed with 615 μl of $CaCO_3$ solution while the rotation speed of the magnetic stirrer was adjusted to 1000 rpm. Afterwards equally 615 μl of the Na_2CO_3 was added and left under invariant stirring conditions for 30 s.
After this precipitation time the glass vial was removed from the magnetic stirrer and the resulting particle suspension was divided into two 1.5 ml tubes. The tubes were left to rest for 3 min at room temperature and afterwards three washing steps with water as well as one with acetone were applied. In each washing step 1 ml of water or acetone were first added to the precipitant. In order to wash the particles and to reduce the aggregation, they were held onto the lab vortex, so that they were mixed with the fluid. For sedimentation of the particles in order to remove the supernatant again, the tubes were centrifuged at 6000 rpm in a centrifuge with a radius of about 5 cm which results in a maximal relative centrifugal force

$$G = \frac{a_z}{g} = \frac{\omega^2 r}{g} = 2012 \tag{7}$$

with g the earths gravitational acceleration. The relative centrifugal force is also called g–force.
After the centrifugation the fluid on top of the precipitant was removed and new water was added to perform the next washing step.
After the washing with acetone the tubes were punctuated with a needle and stored under vacuum for drying.
Three different parameters were analyzed: The impact on the particle size of the temperature, the rotation speed during precipitation as well as the concentration of the stock solutions and Dextran. For each parameter five modulations were chosen and two samples were prepared. The analyzed temperatures were 5 °C, 10 °C, 15 °C, 20 °C and 25 °C. For the different volume concentrations 250 μl, 500 μl, 650 μl, 770 μl and 1000 μl of the aqueous Dextran was used in the synthesis which results in volume concentrations of $0.17\frac{l}{l}$, $0.29\frac{l}{l}$, $0.35\frac{l}{l}$, $0.39\frac{l}{l}$ and $0.45\frac{l}{l}$. As rotation speeds during the precipitation 250 rpm (G=0.35), 500 rpm (G=1.40), 750 rpm (G=3.14), 1000 rpm (G=5.59) and 1200 rpm (G=8.05) were used. For the calculated g–forces a mean rotation radius of 0.5 cm was assumed. Each of these experiments was performed five times and, because of the fluctuations in size, on different days.

3.1.2 Heat shrinking

This experiment was carried out at room temperature if not written otherwise.
For the preparation of the heat shrinking experiments the spherical SiO_2 particles needed to be coated and the cores needed to be removed afterwards, because the shrinking effect only takes place on hollow capsules.
100 μl of SiO_2 particle suspension were washed 5 times with water in order to obtain clean particles for the following coating steps. As coating materials two different systems were used: $(PSS/PDADMAC)_4$ and $(PSS/PAH)_4$.
The solutions of PSS ($2\frac{mg}{ml}$ in 0.5 M NaCl), PAH ($2\frac{mg}{ml}$ in 0.5 M NaCl) and PDADMAC ($2\frac{mg}{ml}$ in 0.5 M NaCl) were prepared with a pH of 6.5. For the adjustment of the pH HCl and NaOH were added.
Because the surface charge of the SiO_2 is negative, it is necessary to start the coating process with the polycation: PAH or PDADMAC. This means, that the last layer is PSS if an even number of layers is applied.
For each layer the particles of one synthesis were suspended in the polyelectrolyte solution (1 ml each time) and left in an sonication bath for two minutes to avoid aggregation. Afterwards they were shaken further ten minutes. Following to this polyelectrolyte exposure the microspheres were sedimented with a centrifuge and the excess of polyelectrolyte was removed. Three washing steps with water followed as described above, before the polyanion was added and the process was repeated.
Following this protocol 4 bilayers of polyelectrolyte were applied.
The cores of the coated particles were then dissolved by using 1 ml of the acid HF in a concentration of 0.3 M. This suspension was agitated and centrifuged several times for 40 min. Afterwards the acid was removed and, in the case that a white sediment remained indicating incomplete core dissolution, new acid was added and the process was repeated until no sediment was visible anymore. Two washing steps with water followed to withdraw the remaining acid.
After this preparation the heat shrinking process could be started. A solution of 10 kDa Dextran fluorescent labeled with FITC in a concentration of 50 μM was added and left one or two hours for incubation at room temperature. During this time the probe was wrapped in aluminum foil in order to protect it from light. In the meanwhile a water bath was heated to 68 °C in which the tubes were placed subsequently for the heating. They were left for 30 min in thermal treatment for the shrinking process protected from light. Afterwards the suspensions were allowed to cool down to room temperature for 5 min and washed twice to remove the non encapsulated FITC-Dextran.
These probes were analyzed with a fluorescence microscope and stored at about 5 °C.

4 Results

4.1 Impact of rotation speed, temperature and concentration on the particle size

In the following diagrams the mean values of each measurement are plotted versus the studied parameter. As error bars the standard deviations of the mean value are used for the measurements in order to make the experiments with different amounts of data comparable: The number of particles measured is for example much smaller if the particles are bigger since the same amount of $CaCO_3$ is available and the area of the microscope picture remains the same. Because of this problem and in order to get a more significant result by reducing the error at least four pictures of each sample were analyzed.
In the following paragraph the analysis of one rotation speed experiment is presented as an example.
After the synthesis the samples were studied under the microscope and pictures were taken from different locations in the sample. In figure 7 a) an original image from the transmission channel of the microscope is shown exemplary. A scale bar was added and the photos were saved in .jpg format.
Afterwards the pictures were processed with ImageJ as described above. The corresponding resulting picture is displayed in figure 7 b).

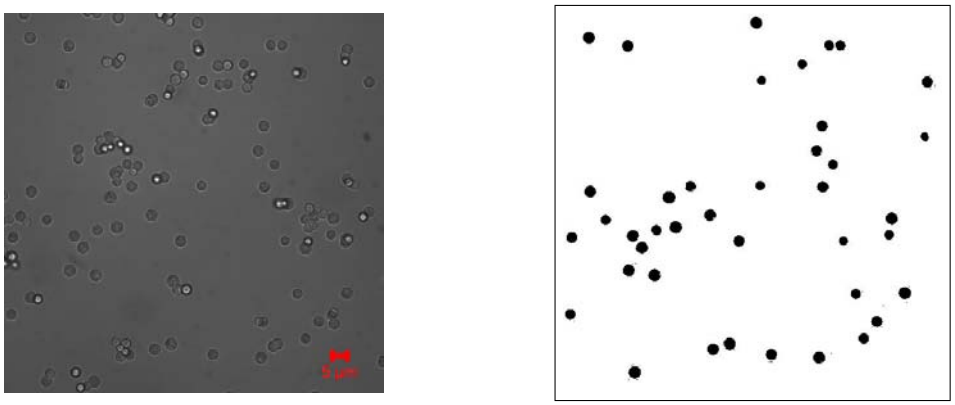

Fig. 7: a) Photo of the particles; b) After processing with ImageJ

ImageJ gives a table as output in which the measured black areas are listed. The scale has been set according to the scale bar in the original image and only those black spots with an area from $1\,\mu m^2$ to $100\,\mu m^2$ were chosen. The resulting tables from all pictures of two equally prepared samples were then combined and the

diameter of the microspheres was calculated according to equation 6. The mean value as well as the standard deviation of the mean value were determined and histograms were generated with the program Origin 6.0. An example is presented in figure 8.

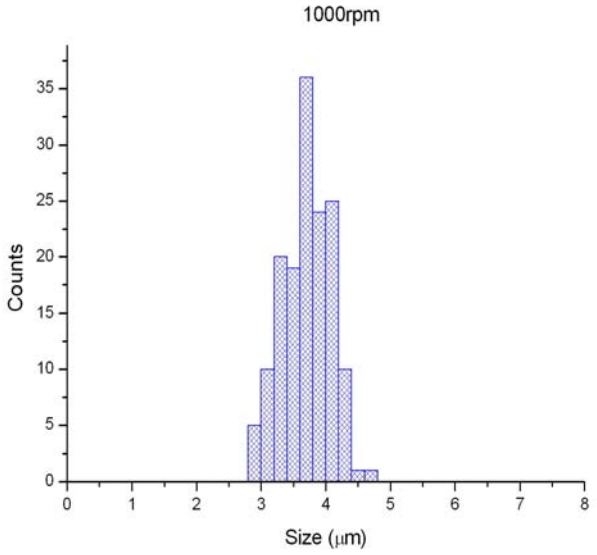

Fig. 8: Histogram of experiment 4, 1000 rpm

Histograms of the other experiments can be found in the supplementary information.

Rotation speed

The Diagram in figure 9 summarizes the data of all experiments in which the rotation speed was variated. The different colors represent the different experiments done and the lines connect the five data points of one experimental series. As ordinate in all three summary graphs the size range 0 μm–7 μm was chosen, in order to make the size changing effect better comparable.

As can be derived from the standard deviation of the mean value the measurements of the different experiments are not identical and in some cases not even comparable, although the same parameter was changed.

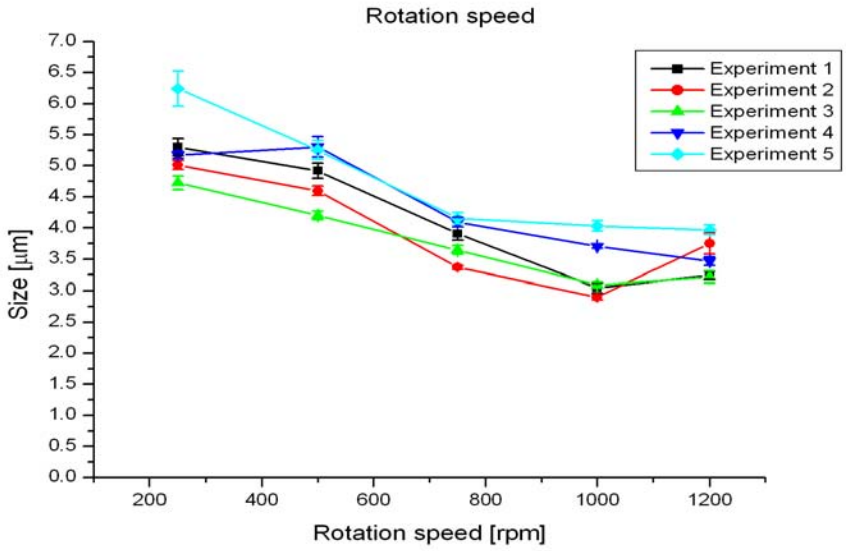

Fig. 9: Variation of the particle size as a function of the rotation speed during synthesis

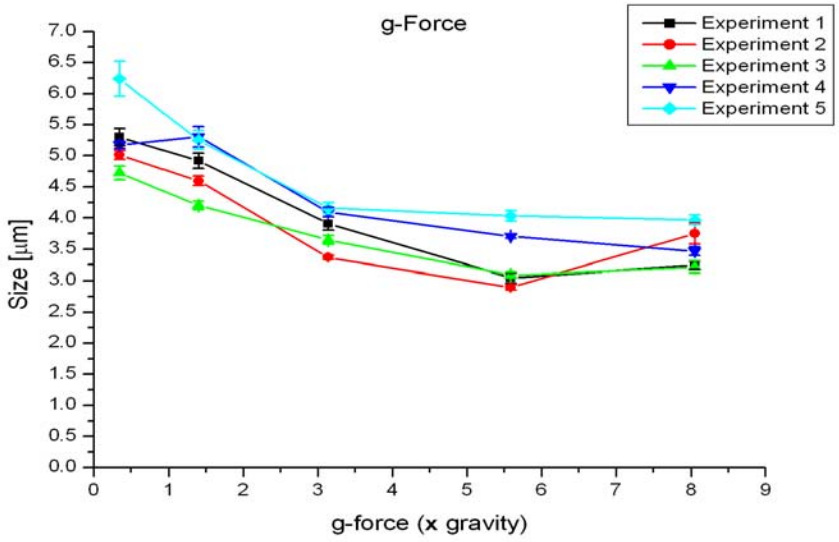

Fig. 10: Variation of the particle size as a function of the effective g-force during synthesis

This can not be explained clearly. It was assumed that another parameter, like for example slight variations in pH of the solutions, has an impact on the precipitation and resulting particle size. This was not further analyzed.
Despite this unexplained variations a clear dependency of the particle size on the rotation speed could be found. By assuming the not understood parameter as constant the gradient of the curve for the experiments was very similar: The mean value of the size became smaller with increasing rotation speed. In the analysis of the rotation speed, especially significant seems to be the effect on the size in the area between 500 rpm and 750 rpm, where the biggest decrease of particle size could be observed resulting in the steepest slope in the figure 9. The reason for the rise in size at the second experiment with the stirring speed of 1200 rpm is the fact, that in one of the two samples the microspheres had a significantly bigger diameter, which influenced the mean value of this experiment. The histogram, that belongs to this experiment is displayed in figure 11. During the rest of the experiments no large difference in size between the two samples was observed. An explanation for this might be, that in the case of the unusual sample there were seed crystals already present in the glass vial or in the pipette tips. If this sample is neglected, the result of this experiment is more similar to the others.

If a mean rotation radius of 0.5 cm for the precipitation is assumed, the resulting g–force that affects the particles can be calculated. In this calculation the radius has an linear impact, so that slight changes in radius do not effect the form of the curve progression. Furthermore the variation of the radius inside the glass vial is the same for all experiments, so that the impact should not change the results. The resulting diagram is show in figure 10. In this figure the particles become smaller with higher g–force as well, because G is proportional to the square of the rotation speed. Nonetheless the curve progression is different: For small g-forces the particle size increases without showing an upper bound in this region.

In the figures 9 and 10 it can be seen, that the mean values of the microspheres size variate in between 6.5 μm and 2.9 μm, if the rotation speed is modulated in the range of 250 rpm–1200 rpm. Although this is a big difference in size, the maximum difference with equal parameters is 1.6 μm which is rather narrow. This means, that a wide range of particle diameters can be reached using this procedure of variating the speed, which is useful for a wide range of applications.

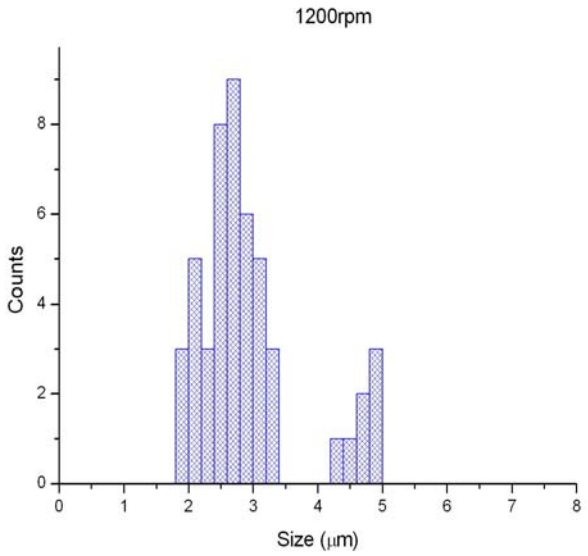

Fig. 11: Histogram of the particle size in the second experimental serie with a rotation speed of 1200 rpm

Temperature

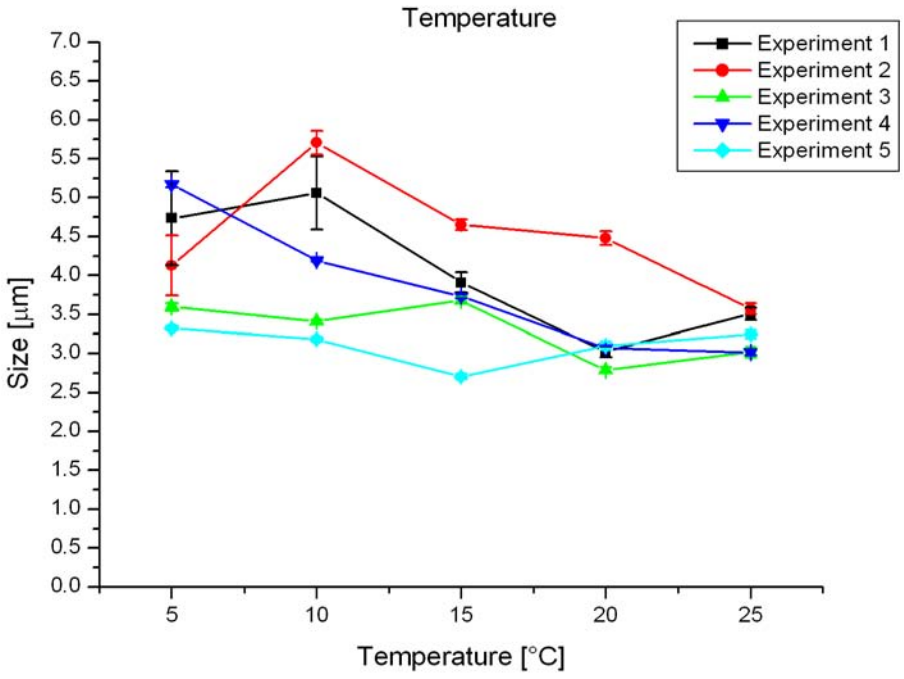

Fig. 12: Variation of the particle size as a function of the temperature

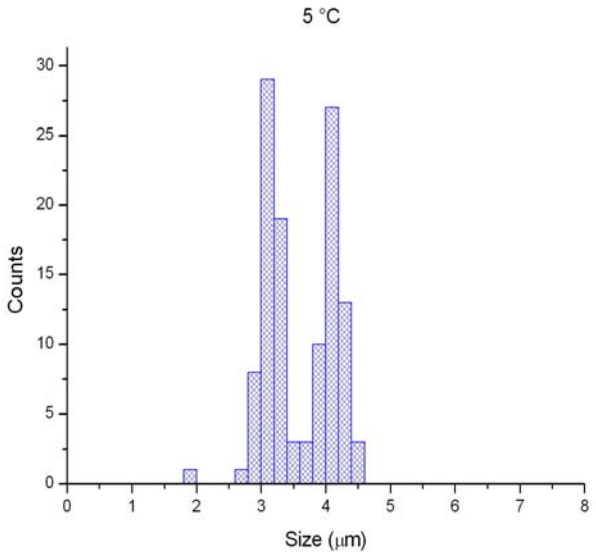

Fig. 13: Histogram of the size variation in the third temperature experiment at 5 °C

In figure 12 the dependency of particle size on the temperature was plotted for all of the five experiments. In comparison with the rotation speed experiment the effect of the temperature seems to be much less predictable, because there was a bigger variance in the resulting gradients for the different experiments conducted. In three of the five experiments a tendency towards smaller particles with higher temperatures could be seen and for the experiment 3 the size is oscillating a little bit, but the general tendency is a decrease in size for warmer solutions. However for the fifth experiment the diameter was the smallest at 15 °C and increased towards the more extreme temperatures. Also the biggest size difference with equal parameters was 2.2 μm which is big compared to the other experiments.
The mean size range was between 2.7 μm and 5.7 μm and hence smaller than in the rotation speed experiment.
If not only the mean values but also the size distribution is studied it stands out, that for the 5 °C measurement of the third experiment the particles in one sample were again significantly bigger than in the other sample. This results in a much smaller mean value. The diagram that is the evidence for that is shown in figure 13.

In the following paragraph some possible reasons for the smaller reproducibility are explained. One of the problems could be, that the temperature was not stable

during the experiment. The solution temperature in the beginning of the synthesis was documented as the experiment temperature. Afterwards the vials were not protected from the room temperature, so that the reaction mixtures became warmer during the precipitation step. Another reason for the observed difference could be, that the initial temperature differed slightly in the compared measurements because the synthesis was not performed immediately after temperature measurement. Also an effect could have been the fact, that the volume of the tempered solutions was not always exactly the same because different amounts of solution were used of aqueous Dextran (770 μl) than of $CaCl_2$ and Na_2CO_3 (615 μl) for each synthesis. Therefore the temperature was not exactly the same for all of the solutions.
For the synthesis of $CaCO_3$ particles at very low temperatures around 5 °C a further observation was made: If the temperature was particularly low the $CaCO_3$ was not sedimented during centrifugation but remained in the solution as a cloudy suspension. Only after several washing steps and with the gradual warming of the suspension, the precipitant was formed. In those samples the size distribution was especially wide: The cloudy solution was stable even after the 30 s resting time for Experiment 1 (0 °C and 6.5 °C) and 2 (5 °C).
Nonetheless it could be shown, that in general the size range was larger when the temperature was lower. At lower temperatures bigger microspheres were produced although some very small particles remained in the suspension as well.
In order to produce bigger particles the effect of lower temperature could be used. The comparatively big size range can be decreased after synthesis by using sedimentation of the bigger particles via centrifugation.

Concentration

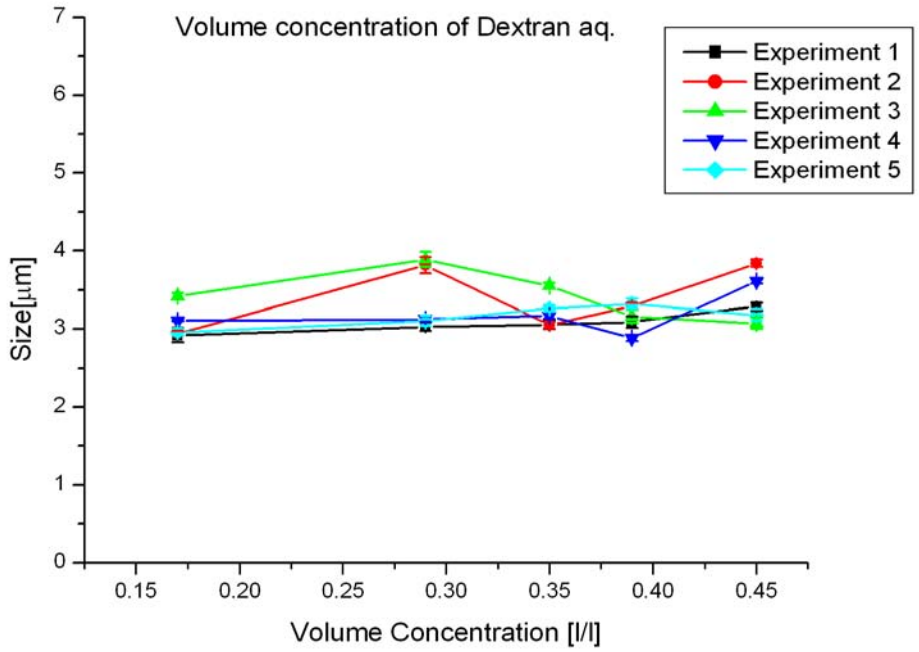

Fig. 14: Variation of the particle size as a function of the Dextran aq. volume concentration during precipitation

In the volume concentration experiment the size variation was the smallest: In all the experiments the sizes ranged between 2.9 μm and 3.9 μm with a size distribution of 0.9 μm at a constant parameter. This variation in size is even smaller than the difference between equal parameters for the temperature experiment, which makes this effect irrelevant in comparison to the unknown size effect responsible for the variation between the experiments. Especially the measurements in experiment one and five are nearly constant in diameter. In all experiments except the third one, there was a very small rise in size between the 250 μl data and the 1000 μl measurement. This could mean, that with a higher Dextran concentration during the synthesis also more Dextran is enclosed in the microspheres. Besides this effect the size range is the narrowest at a volume concentration around 0.39 $\frac{l}{l}$, the concentration used in the traditional routine. For this concentration 770 μl of aqueous Dextran was used.

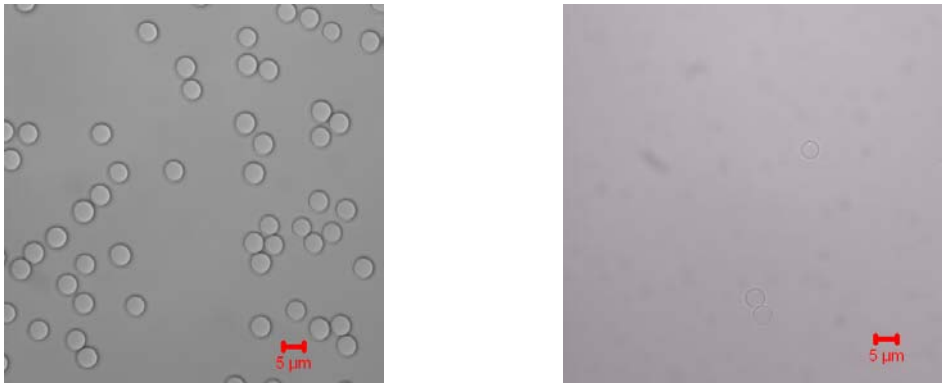

Fig. 15: a) The coated SiO_2 particles; b) After core dissolution with HF

Other than that the volume concentration seems to have no impact on the size distribution.

4.2 Post–loading of polyelectrolyte capsules prepared on SiO_2 templates via heat shrinking

In the following images the $(PAH/PSS)_4$ and $(PDADMAC/PSS)_4$ capsules prepared on SiO_2 templates are shown at the different production steps as well as after the loading with FITC-Dextran.

PAH/PSS

In figure 15 a) the coated microspheres are shown. They are rarely aggregated, monodisperse and present in abundant number. But during the washing steps for the core dissolution the particle number decreased drastically and the particle aggregation increased. Also the layering appeared rather fuzzy under the microscope – the samples were not as spherical any more.
The challenge in this step is the complete removal of the template material. But this seems to happen much slower than expected because of the multilayer coating. Furthermore there was a hight loss of capsules because of the washing steps during and after dissolution
After the core seemed to be removed successfully, the heat shrinking procedure was carried out as described in the section methods. The figure 16 shows some capsules after the heat shrinking in an image divided into fluorescence channel, transmission channel and the corresponding merged image. It can be seen, that the resulting effect was not the same for all of the particles: Two out of the three

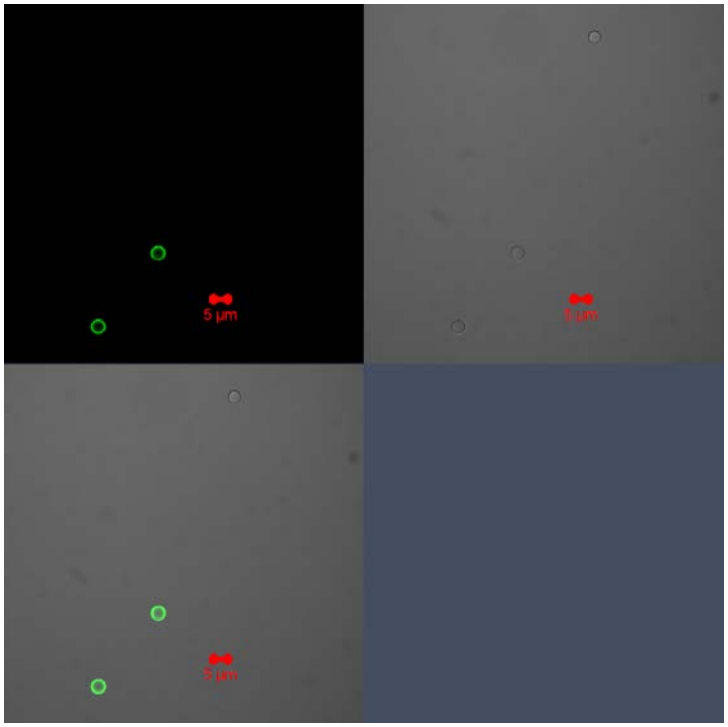

Fig. 16: PAH/PSS capsules after the heat shrinking and loading

capsules in the image were fluorescently labeled while a third one showed no fluorescence. By analyzing the size of the fluorescent and non fluorescent capsules it was observed, that the non fluorescent capsules were even bigger in diameter than before the thermal treatment and that the fluorescent capsules were shrunk between 5 % and 16 %. In the samples with capsules coated with PAH/PSS about 91 % of the analyzed capsules were fluorescent.
The fluorescent capsules had mainly a fluorescent ring structure under the microscope. This suggests, that the FITC–Dextran was caught in between the polyelectrolyte layers and either did not enter the cavity at all or could not be reliably kept inside the capsule.

PDADMAC/PSS

The System (PDADMAC/PSS) showed in the first two steps no difference to the system (PAH/PSS): Because of the core removal the capsules became fewer, more aggregated and less spherical.

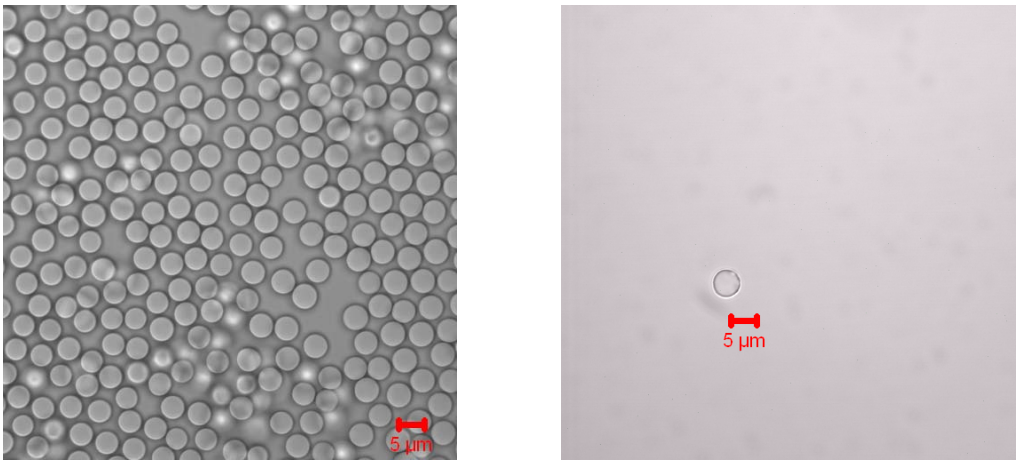

Fig. 17: a) The PDADMAC/PSS coated SiO_2 particles; b) After core dissolution

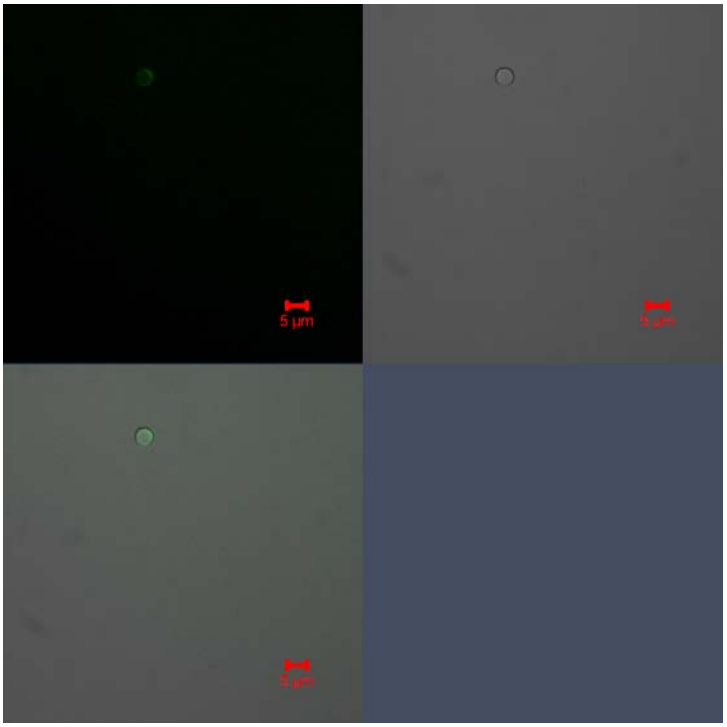

Fig. 18: PDADMAC/PSS capsules after the heat shrinking and loading

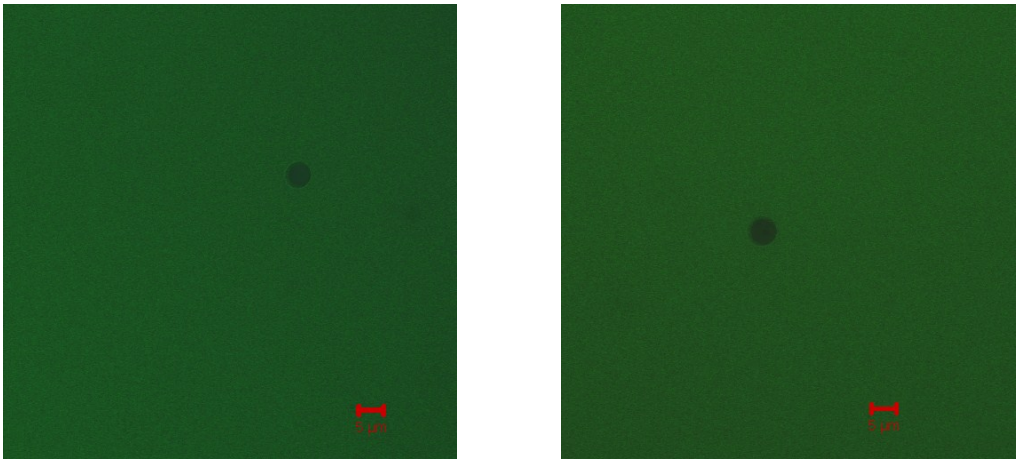

Fig. 19: a) PAH/PSS capsules during incubation; b) PDADMAC/PSS capsules during incubation

After the heat shrinking procedure not all of the particles were labeled with FITC-Dextran: several particles were either not fluorescent or only a little bit on the outmost edge. In this experiment much less PDADMAC/PSS capsules remained and only 14 % of the remainig capsules were clearly fluorescent. Some of the rest had a thin fluorescent boundary that could not always be distinguished.
Moreover the shrinking process was not as reliable in this experiment as for the PAH/PSS capsules: some capsules were swelling instead of shrinking during the heat treatment. This is not compatible with the expectations according to the literature.
Capsules that were fluorescent showed a much higher fluoresceine concentration in the polyelectrolyte layers than in the capsule cavity.

Analysis of the problem in the heat shrinking procedure

In order to find out, whether the Dextran enters the cavity during the incubation, pictures were taken during the incubation time with Dextran-FITC. In both, the PAH/PSS system and the PDADMAC/PSS system, the Dextran could not be found inside the cavity, even if the incubation time was elongated to two hours. Two representative images can be found in figure 19. In the pictures the green fluorescent Dextran–FITC can be seen with two black circles that are the polyelectrolyte capsules. This is evidence, that the Dextran–FITC with a molecular weight of 10 kDa is not able to diffuse in the capsules cavity, since there is no green fluorescent inside.
This is unexpected because the polyelectrolyte walls should not be too tight for

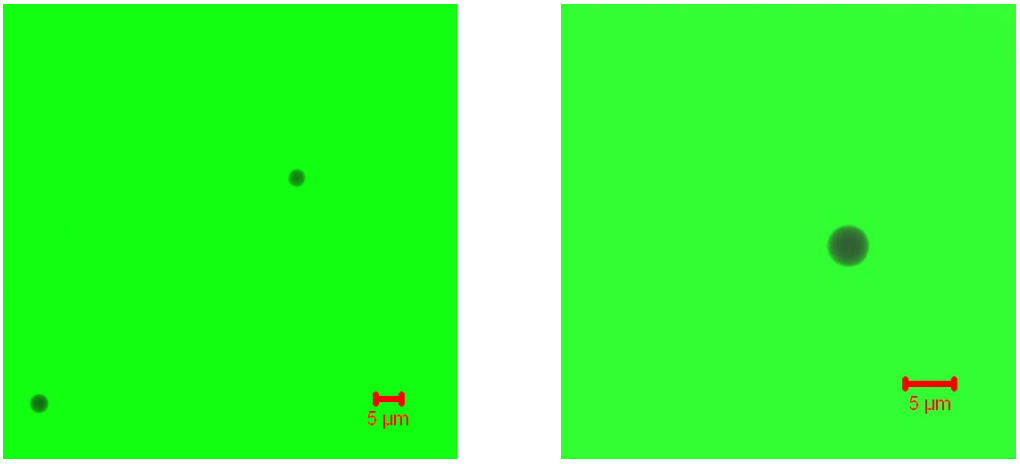

Fig. 20: a) PAH/PSS capsules with free fluorescent; b) PDADMAC/PSS capsules with free fluorescent

particles of this low molecular weight to enter. In the literature even particles with higher molecular weight of 10 kDa and more have been reported to be enclosed following this procedure. Maybe the reason for this problem is, that a small amount of the core is left so that a repulsive potential remains. In order to find out, if the capsules are impermeable for even smaller particles, free fluorescien has been tried to encapsulate. The pictures 20 show the results after one hour. Again for most capsules no encapsulation could be seen: The capsules appear as black circles in the fluorescence channel, which means that the intensity of the fluorescence is much lower inside the capsules.
This confirms the interpretation, that there is a further problem with the produced capsules like remains of the SiO_2 core, that induce a repulsive potential.
For a successful encapsulation this needs to be analyzed further.

5 Discussion and Outlook

The research on this interface of physics, chemistry, material science and biology is much less based on theoretical equations than other fields of physics. This results sometimes in a different approach to problems. Often the principles are first analyzed empirically before the theoretical model follows. In the two areas, that were tried to optimize in this work, the first topic of calcium carbonate precipitation has been subject to research for a rather long time and some models to describe it exist. Despite this, the reproducibility is still limited because the conditions in the lab change continuously: The climate changes, the composition of the surrounding air, the experimental tools were not sterile and other experiments have been conducted alongside. These reasons as well as the fact that the clustering of the vaterite particles and of particles with amorphous $CaCO_3$ is a statistical effect could have an impact on the measurements. This clustering is not yet calculable. This might explain why the results measured are not always very predictable.
The second field of study, the post loading of capsules, on the other hand is a new topic researched only for a few years until now. Some theories exist about why the shrinking takes place for one of the systems, but for the next one it does not apply any more. Because of this and for the reason of its applicability it would be interesting to improve this loading method to make it simple and reproducible. Although an ideal optimization of the synthesis and loading process was not achieved, some helpful tendencies and better defined problems were achieved:

5.1 Rotation speed

Although a prediction of the particle size by adjusting the known parameters is not possible yet, at least the size can be influenced by changing the rotation speed after the size is measured for one synthesis. This pilot synthesis is necessary, to find out the impact of the unknown parameter.
Because the rotation speed is such a nice tunable parameter and relatively reproducible this technique could thus be standardized. It would therefore be interesting to analyze the rotation speed in smaller intervals with the goal to find the mathematical dependency. After a pilot synthesis has been done this could be used to calculate the rotation speed needed to produce the desired size under otherwise constant parameters. This would also help to understand the crystallization process much better.

5.2 Temperature

The effect of a temperature change was not as predictable as for the rotation speed. For low temperatures around 10 °C in general bigger particles than with higher temperatures of 25 °C occurred, but in some cases there was also a rise in size towards the synthesis with warmer solutions. What can be said is, that precipitation at low temperature leads to a wider range is size and thus would make a further isolation of a certain particle size necessary for gaining monodisperse templates. At temperatures close to 0 °C this effect was especially significant. This became obvious during the synthesis, because of the quite stable cloudy suspension, which makes this procedure less predictable and less suitable for standardized production.

5.3 Concentration

The volume concentration of the solutions during the synthesis seemed to have a negligible impact on the particle size. This might mean, that a bigger amount of the cargo can be loaded without increasing the diameter in a way resulting into to big capsules.
At this point it would be interesting to study on the one hand, how much of Dextran was internalized in the particles. This could be quantified by labeling the Dextran for example with a fluorescent dye and to measure and compare the fluorescence levels after synthesis.
On the other hand it would be interesting to find out how much importance the molecular weight and charge of the incorporated cargo has. The Dextran used had a molecular weight of 2000 kDa but it can be expected, that smaller molecules would result in smaller particles. This could be an interesting study for further research.

5.4 Heat shrinking

In this study it was possible to produce a few non aggregated and spherical polyelectrolyte capsules of the systems PAH/PSS and PDADMAC/PSS. These capsules could then be labeled, but not filled with Dextran–FITC and treated with heat. Other than it has been reported in the literature, the shrinking effect of the PDADMAC/PSS capsules was not reliable since some of the capsules swelled instead. Also the main amount of Dextran–FITC was not inside the capsule cavity, from which it could be released in a controlled way, but in the capsule walls.

A reason for these problems might be a non constant temperature in the water-bath, a too short annealing time or a too short incubation time of one hour. These parameters could further be variated to archive a loading of the capsule cavity instead of walls. Furthermore other molecular weights could be used to find the cutoff in which the Dextran can not enter the capsules any more and in which the Dextran can not be kept inside at all. Moreover it would be useful to understand quantitatively how much has been loaded into the cavity by this method under the conditions given.
Because even for free dye and after a long incubation time the fluorophors did not permeate the walls of all capsules, it would be interesting to increase the dissolution time and HF amount to make sure, that all of the core is dissolved.

Conclusion

A definite effect on the size was only found out for the rotation speed. The particle size became smaller with higher rotation speed during the synthesis. For the temperature there might be a dependency, but further measurements would be necessary. The concentration of cargo material does not seem to have a relevant effect on the particle size.
For the heat shrinking the production of capsules was accomplished, but Dextran did not enter the cavity but got caught in the walls. Also the shrinking effect was only partly verified.

Acknowledgments

I would like to express special thanks to Prof. Dr. Wolfgang J. Parak, who gave me the opportunity of doing this thesis in his biophotonics group. Because of his support, the interesting topic and the given room to pursue my own ideas, it was a pleasure to do this bachelor thesis despite the difficult surrounding conditions in the beginning. Also I would like to thank Prof. Dr. Kerstin Volz for agreeing to be the second assessor.
I would like to thank Carolin Ganas for her supervision and support as well as proof reading of my thesis and Markus Ochs who took the time to introduce me to the lab techniques.
During the past few months I was supported constantly from the members of the biophotonics group, who helped me especially in all chemistry related fields.
Finally I would like to thank my family and my friends, especially my parents, my sister Dorothea and my boyfriend Jan.

References

[1] G. Decher [1997]. 'Fuzzy nanoassemblies: Toward layered polymeric multicomposites'. Science 277 1232-1237

[2] J. Schlenoff, S.Dubas [2001]. 'Mechanism of Polyelectrolyte Multilayer Growth: Charge Overcompensation and Distribution'. Macromolecules 34 592-598

[3] P.Rivera Gil, L.L.del Mercato, P.del_Pino, A. Munzos_Javier, W.J.Parak [2008]. 'Nanoparticle-modified polyelectrolyte capsules'. Nano Today 3 12-21

[4] F.Caruso, H. Lichtenfeld, M. Giersig, H. Möhwald [1998]. 'Electrostatic Self-Assembly of Silica Nanoparticle-Polyelectrolyte Multilayers on Polystyrene Latex Particles'. J. Am. Chem. Soc. 120(33) 8523-8524

[5] D. V. Volodkin, N. I. Larionova, G. B. Sukhorukov [2004]. 'Protein Encapsulation via Porous CaCO3 Microparticles Templating'. Biomacromolecules 5 1962-1972.

[6] A.Voinescu [2008]. 'Biomimetic Formation of CaCO3 Particles Showing Single and Hierarchical Structures'. 16

[7] D.V.Volodkin, A.I.Petrov, M.Prevot, G.B.Sukhorukov [2004]. 'Matrix Polyelectrolyte Microcapsules: New System for Macromolecule Encapsulation'. Langmuir 20 3398-3406

[8] S.Wilhelm, B.Gröbler, M.Gluch, H.Heinz. 'Confocal Laser Scanning Microscopy'. 3

[9] G.B.Sukhorukov, A.Fery, M.Brumen, H.Möhwald [2004]. 'Physical chemistry of encapsulation and release'. PCCP 6 4078-4089

[10] G.B.Sukhorukov, D.V.Volodkin, A.M. Günther, A.I.Petrov, D.B.Shenoy, H.Möhwald [2004]. 'Porous calcium carbonate microparticles as templates for encapsulation of bioactive compounds'. J. of Mat. Chem. 14 2073-2081

[11] A.Voigt, N.Buske, G.B.Sukhorukov, A.A.Antipov, S.Leporatti, H.Bäumler, E.Donath, H.Möhwald [2001]. 'Novel polyelectrolyte multilayer micro- and nanocapsules as magnetic carriers'. Journal of Magnetism and Magnetic Materials 225 59-66

[12] A.A.Antipov, G.B.Sukhorukov, E.Donath, H.Möhwald [2000]. 'Sustained Release Properties of Polyelectrolyte Multilayer Capsules'. J.Phys. Chem. 105 2281-2284

[13] A.A.Antipov, G.B.Sukhorukov, Y.A. Fedutik, J. Hartmann M. Giersig, H. Möhwald [2002]. 'Fabrication of a Novel Type of Metallized Colloids and Hollow Capsules'. Langmuir 18 6687-6693

[14] Y.Lvov, A.A.Antipov, A.Mamedov, H.Möhwald, G.B.Sukhorukov [2001]. 'Urease Encapsulation in Nanoorganized Microshells'. Nano Letters 3 125-128

[15] O.P.Tiourina, A.A.Antipov, G.B.Sukhorukov, N.I.Larionova, Y.Lvov, H.Möhwald [2001]. 'Entrapment of a-Chymotrypsin into Hollow Polyelectrolyte Microcapsules' Macromol. Biosci. 1 209-214

[16] Xiaoling Yang, Xiao Han, Yihua Zhu [2005] $(PAH/PSS)_5$ microcapsules templated on silica core: Encapsulation of anticancer drug DOX and controlled release study

[17] S.J.Parkin, R.Vogel, M.Persson, M.Funk, V.L.Y.Loke, T.A.Nieminen, N.R.Heckenberg, H.Rubinsztein-Dunlop [2009]. 'Highly birefringent vaterite microspheres: production, characterization and applications for optical micromanipulation'. Optics express Vol. 17 No. 24 21944-21955

[18] J.Yu, H.Guo, S.A.Davis, S.Mann [2006]. 'Fabrication of Hollow Inorganic Microspheres by Chemically Induced Self-Transformation'. Advanced Functional Materials 16 15 2035 - 2041

[19] K.Sawada [1997].'The mechanisms of crystallization and transformation of calcium carbonates'. Pure & Appl. Chem., Vol. 69, No. 5, 921-928

[20] Feng-Wen Yan, Shu-Feng Zhang, Cun-Yue Guo, Xiao-Hui Zhang, Guo-Chang Chen, Fang Yan, Guo-Qing Yuan [2009]. 'Influence of stirring speed on the crystallization of calcium carbonate'. Cryst. Res. Technol. 44, No. 7, 725-728

[21] M.Faatz [2004]. 'Kontrollierte Fällung von amorphem Calciumcarbonat durch homogene Carbonatfreisetzung'. Dissertation. p.59-63

[22] C.Ganas [2010]. 'Beladung von Polyelektrolytmikrokapseln mit Polyethylenimin und Desoxyribonukleinsäure'. Diplomarbeit

[23] C.Y.Gao, S.Leporatti, S.Moya, E.Donath, H.Möhwald [2003].'Swelling and Shrinking of Polyelectrolyte Microcapsules in Response to Changes in Temperature and Ionic Strength' Chemistry-A European Journal 9 915

[24] K.Köhler, D.G.Shchukin, H.Mohwald, G.B.Sukhorukov [2005]. 'Thermal Behavior of Polyelectrolyte Multilayer Microcapsules. 1. The Effect of Odd and Even Layer Number'. Journal Of Physical Chemistry B 109, 18250.

[25] K.Köhler, H.Möhwald, G.B.Sukhorukov [2006].'Thermal Behavior of Polyelectrolyte Multilayer Microcapsules: 2. Insight into Molecular Mechanisms for the PDADMAC/PSS System'. JOURNAL OF PHYSICAL CHEMISTRY B 110 24002.

[26] M.J.McShane, J.Q.Brown, K.B.Gulce, Y.M.Lvov [2002]. Polyelectrolyte Microshells as Carriers for Fluorescent Sensors: Loading and Sensing Properties of a Ruthenium-Based Oxygen Indicator

[27] S.Leporatti, C.Gao, A. Voigt, E.Donath, H.Möhwald [2001], 'Shrinking of ultrathin polyelectrolyte multilayer capsules upon annealing: A confocal laser scanning microscopy and scanning force microscopy study', The European Physical Journal 5 13-20

[28] K.Köhler, G.B.Sukhorukov [2007]. 'Heat Treatment of Polyelectrolyte Multilayer Capsules: A Versatile Method for Encapsulation'. Advanced Functional Materials 17 2053-2061

[29] A.M.Javier, P.del Pino, M.F.Bedard, D.Ho, A.G.Skirtach, G.B.Sukhorukov, C.Plank, W.J.Parak [2008]. 'Photoactivated Release of Cargo from the Cavity of Polyelectrolyte Capsules to the Cytosol of Cells'. Langmuir 24 12517-12520

[30] W.Song, Q.He, H.Möhwald, Y.Yang, J.Li [2009]. 'Smart polyelectrolyte microcapsules as carriers for water-soluble small molecular drug'. Elsevier doi:10.1016/j.jconrel.2009.06.010

[31] G.Ibarz, L.Dähne, E.Donath, H.Möhwald [2002]. 'Controlled permeability of Polyelectrolyte Capsules via Defined Annealing'. Chem. Mater. 14 4059-4062

List of Figures

Supplementary Information

Experiment 1: Variation of the Dextran aq. amount

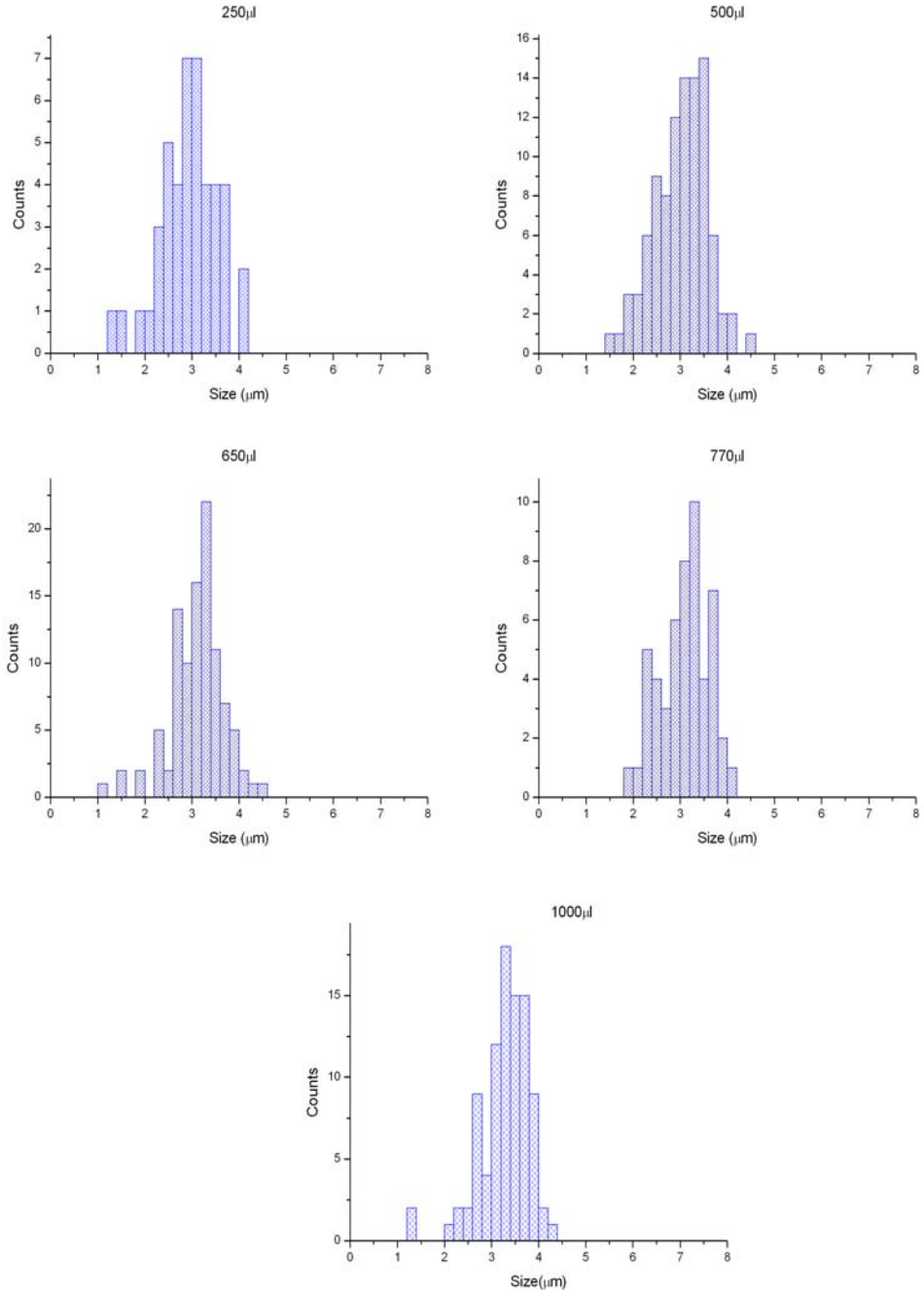

Experiment 2: Variation of the Dextran aq. amount

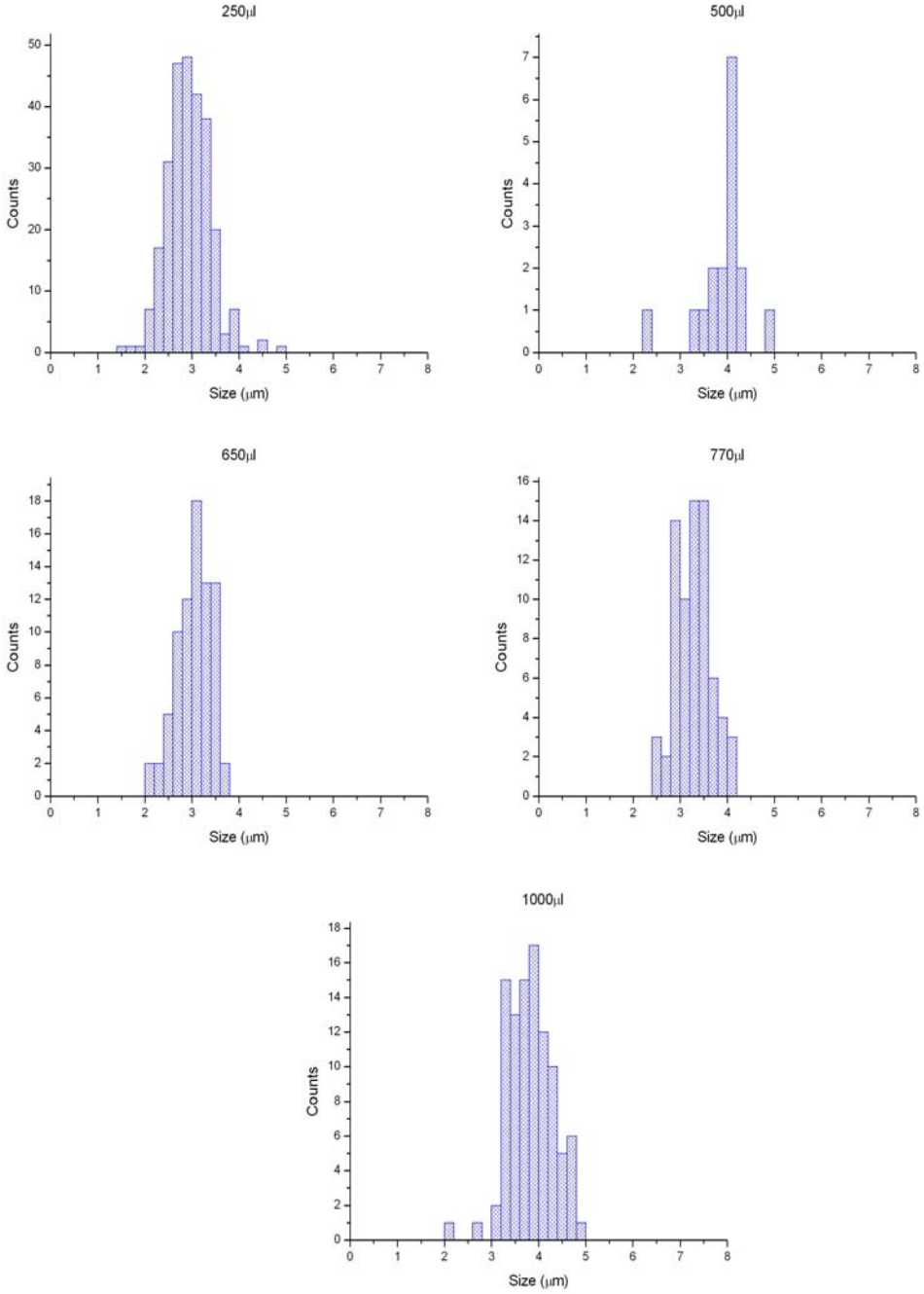

Experiment 3: Variation of the Dextran aq. amount

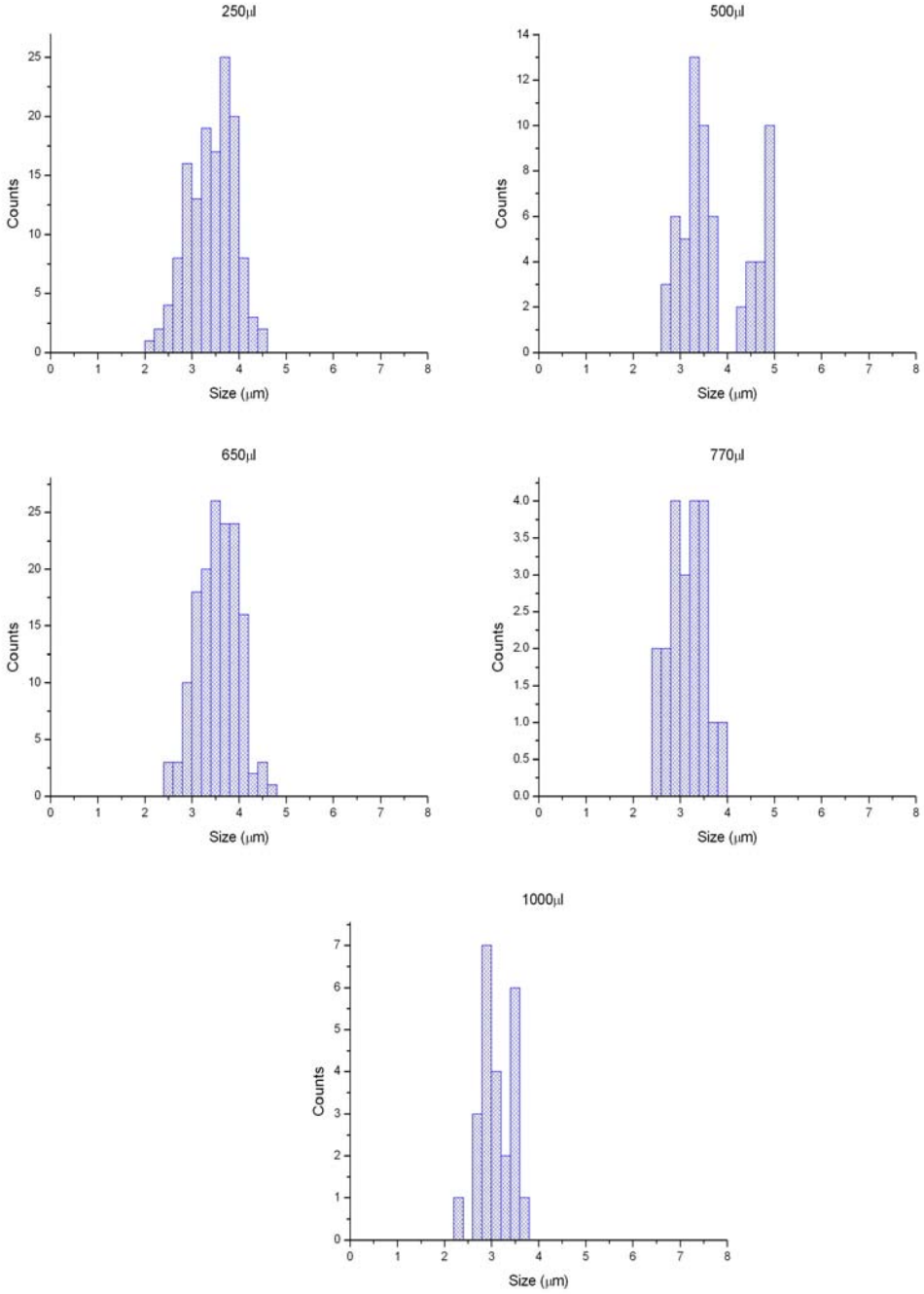

Experiment 4: Variation of the Dextran aq. amount

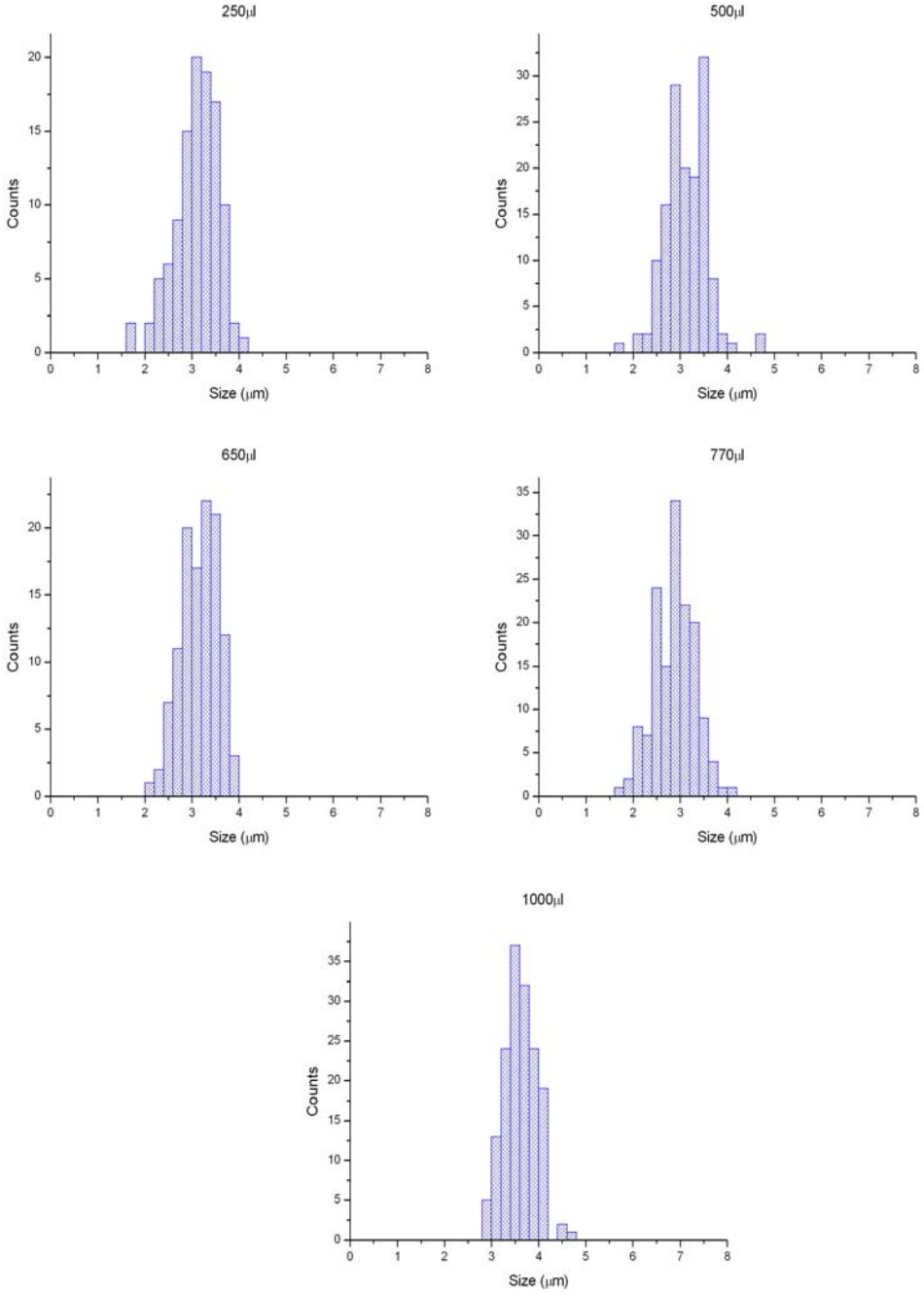

Experiment 5: Variation of the Dextran aq. amount

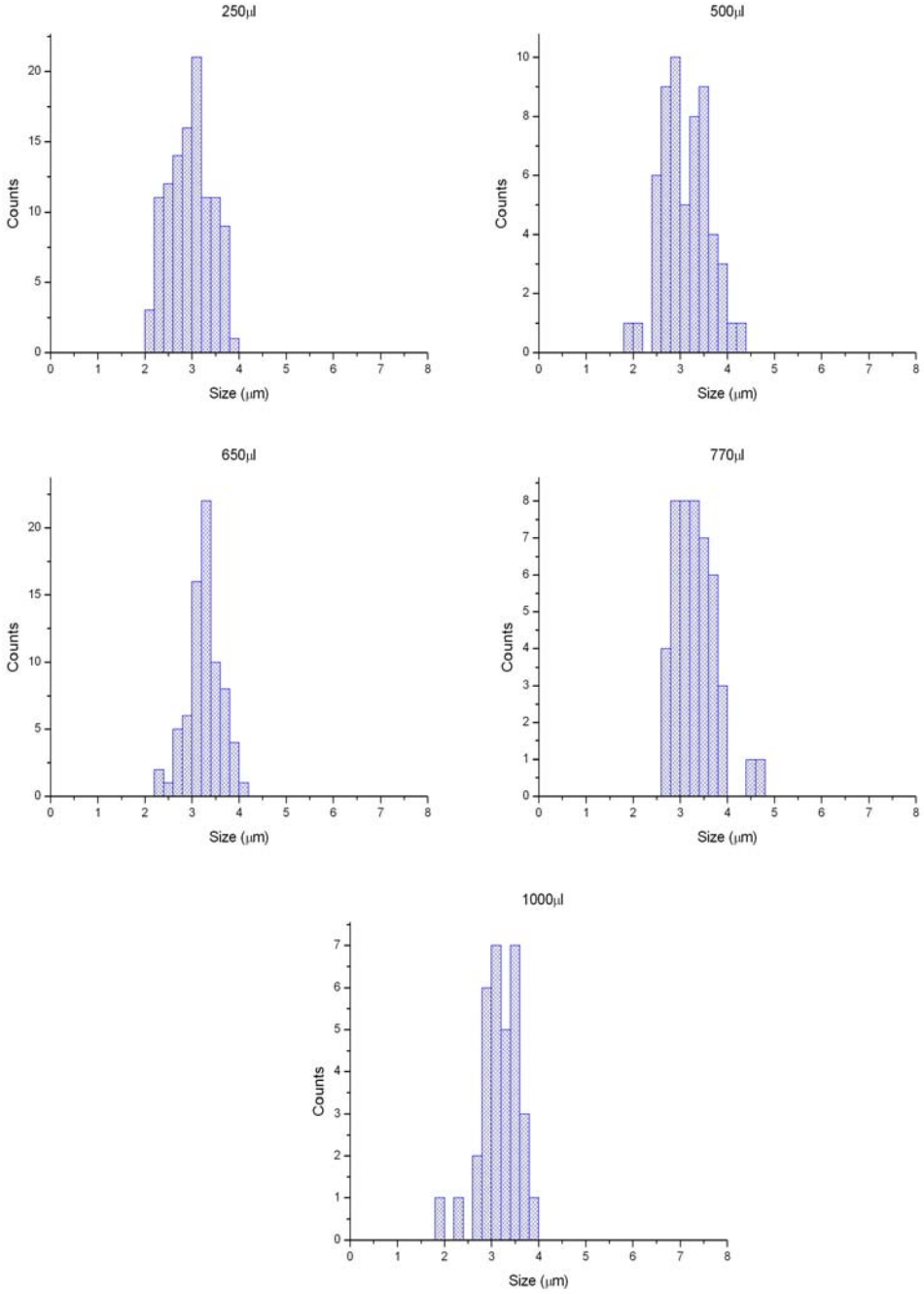

Experiment 1: Temperature

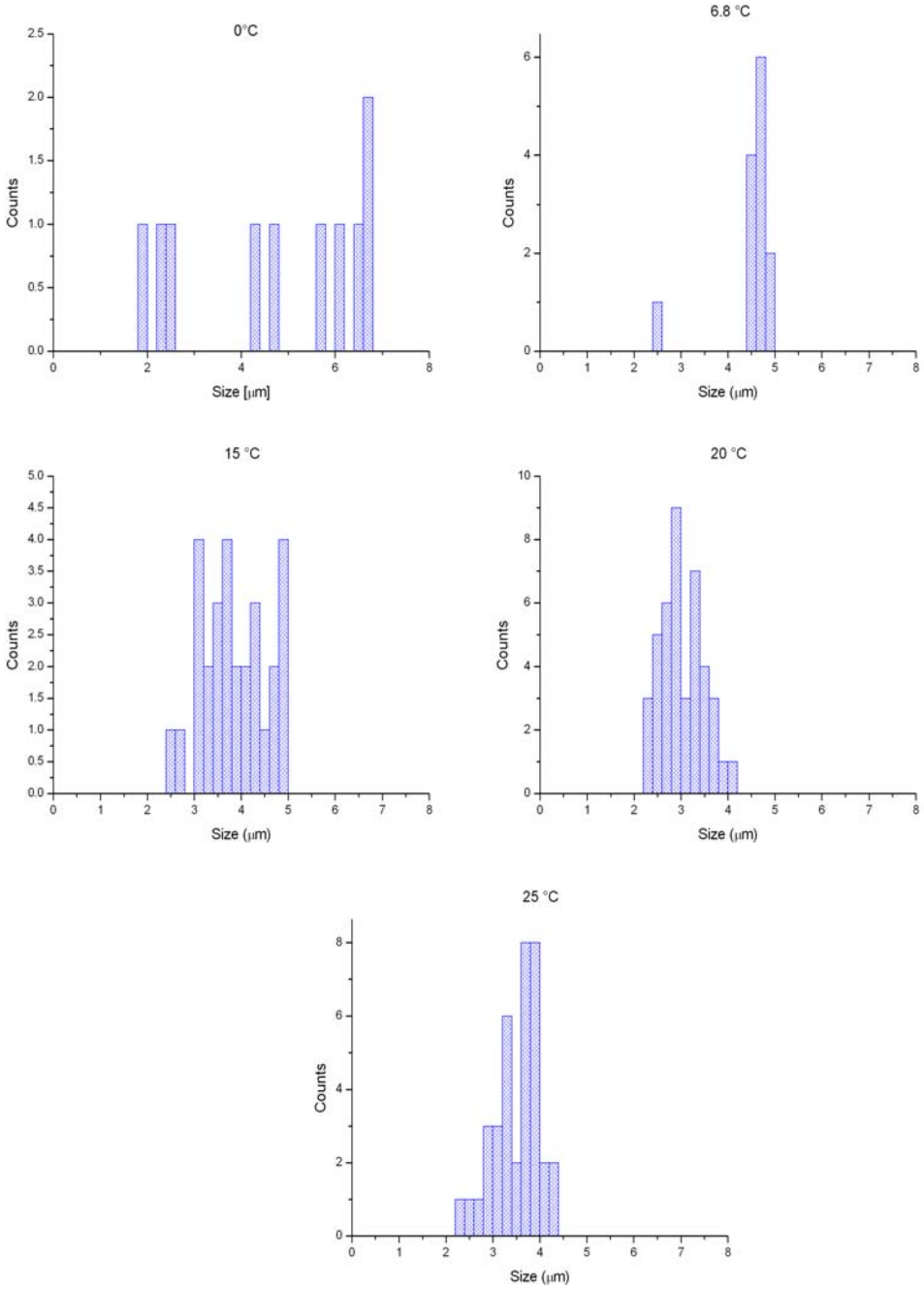

Experiment 2: Temperature

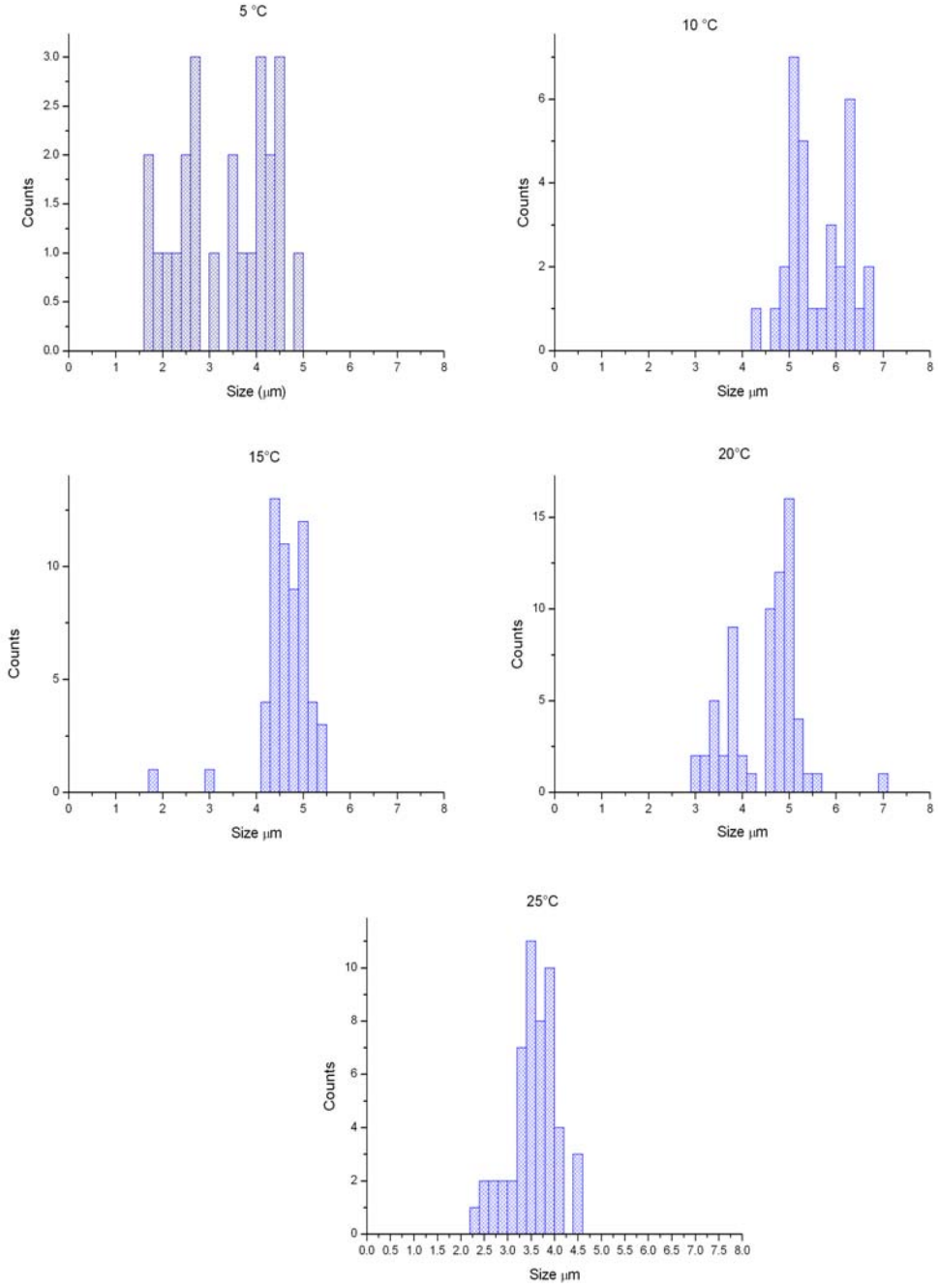

Experiment 3: Temperature

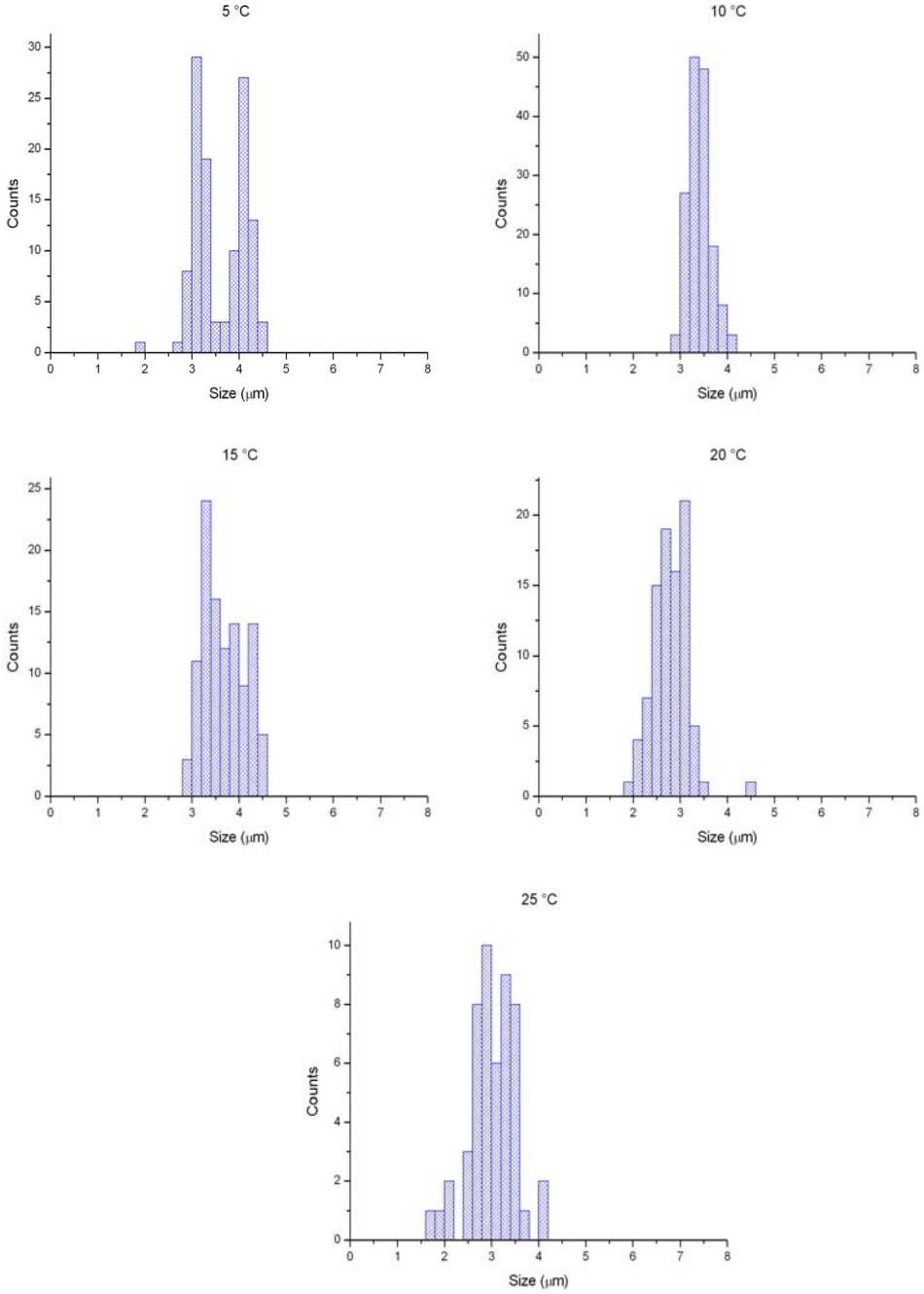

Experiment 4: Temperature

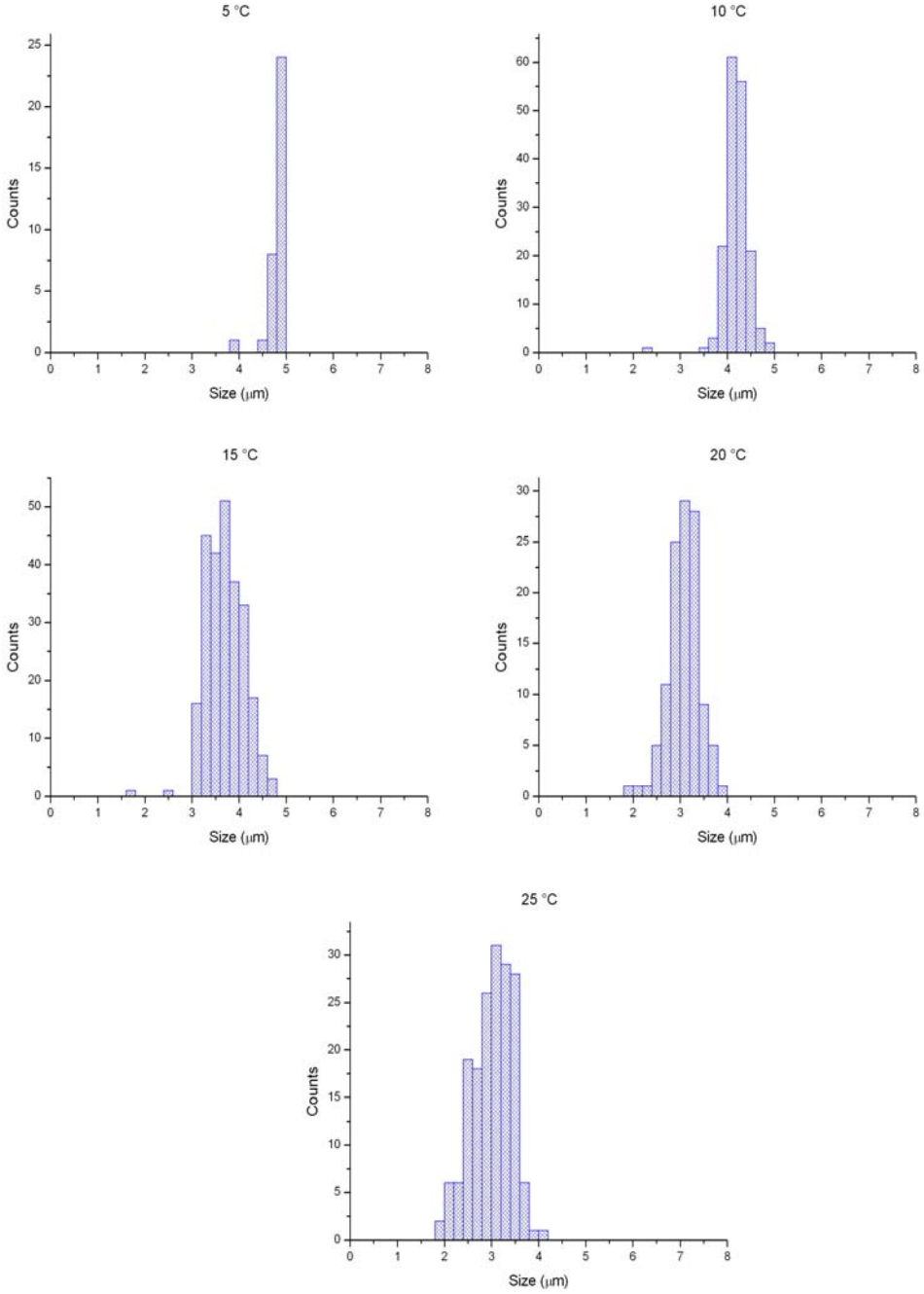

Experiment 5: Temperature

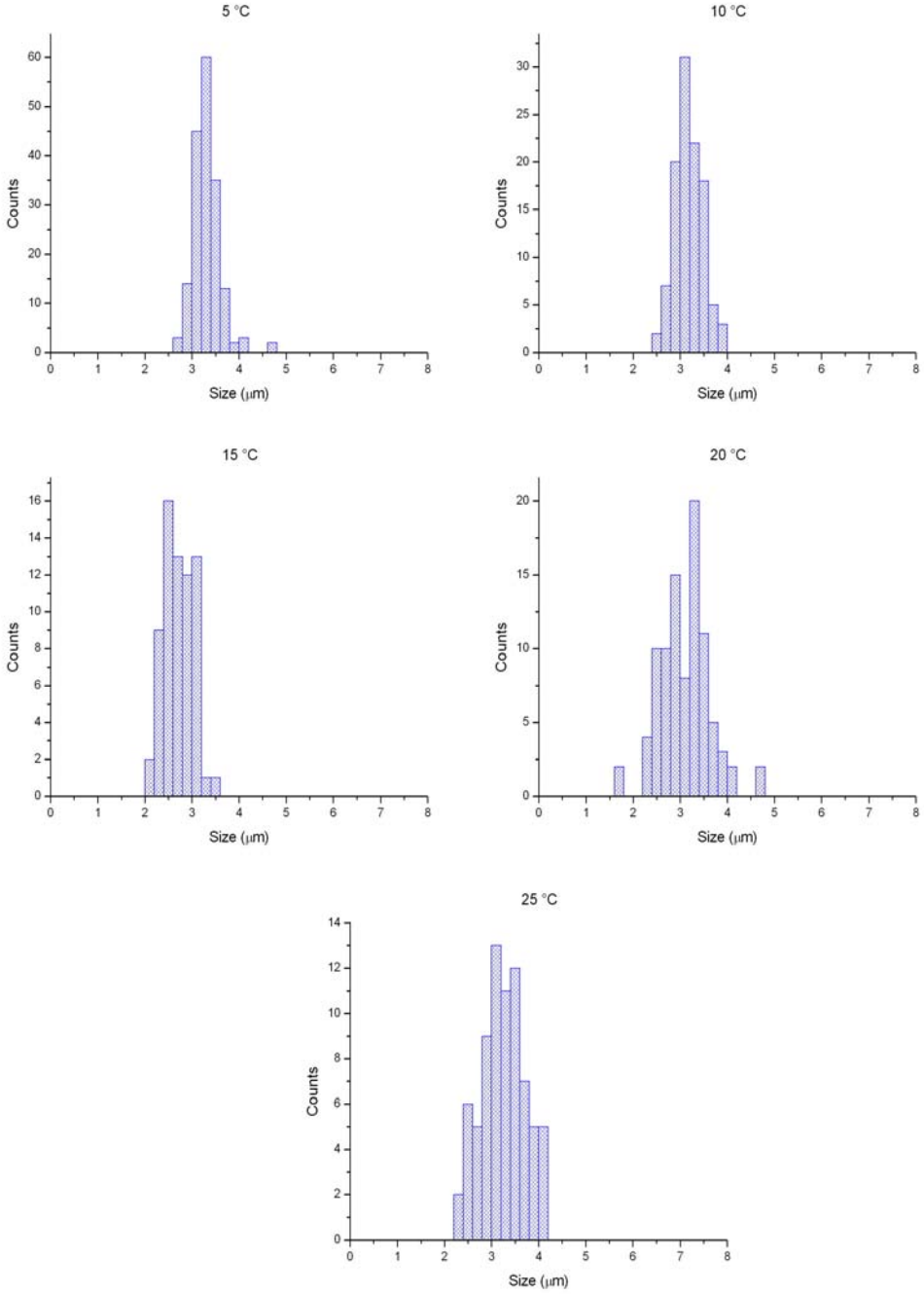

Experiment 1: Rotation speed

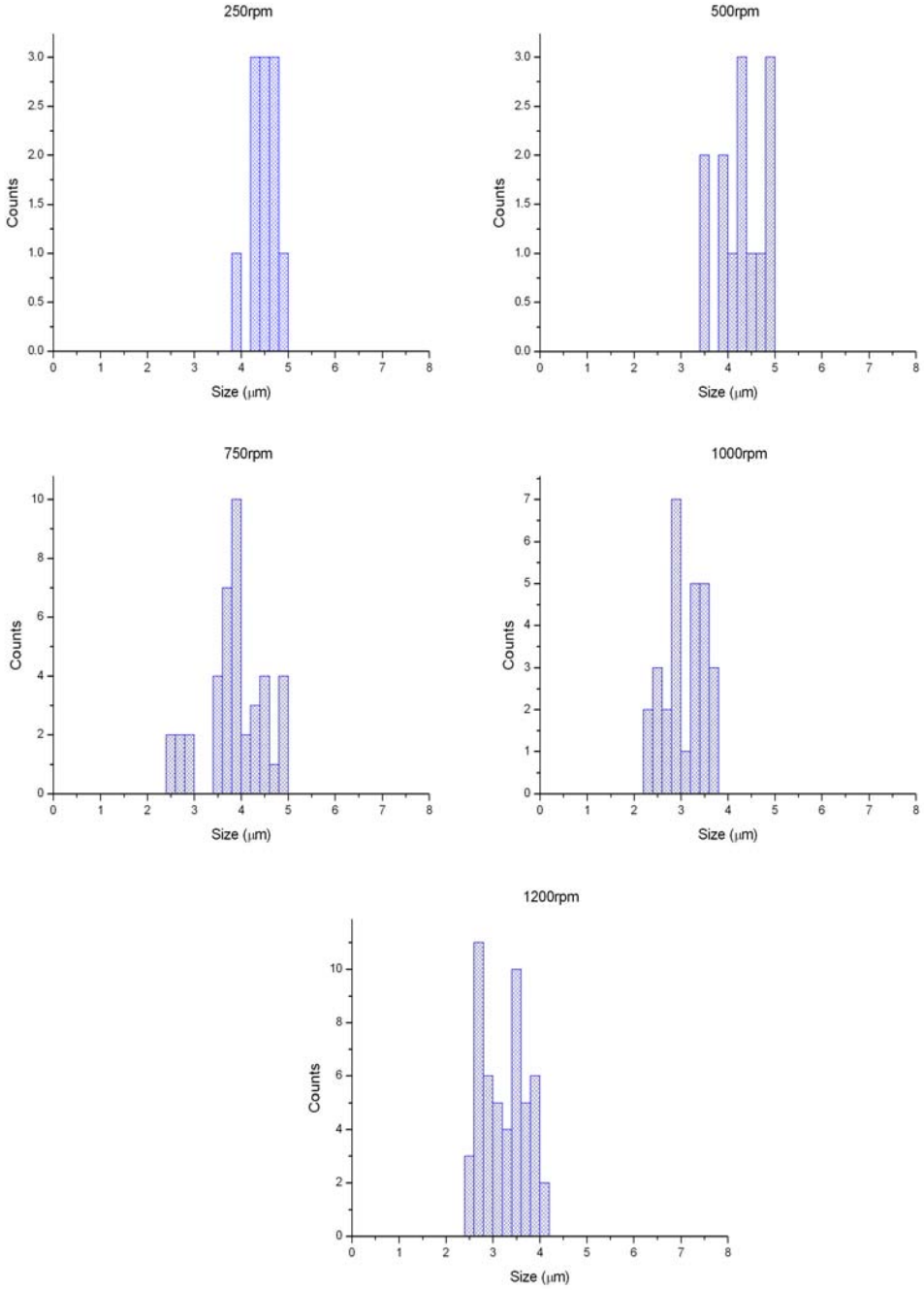

Experiment 2: Rotation speed

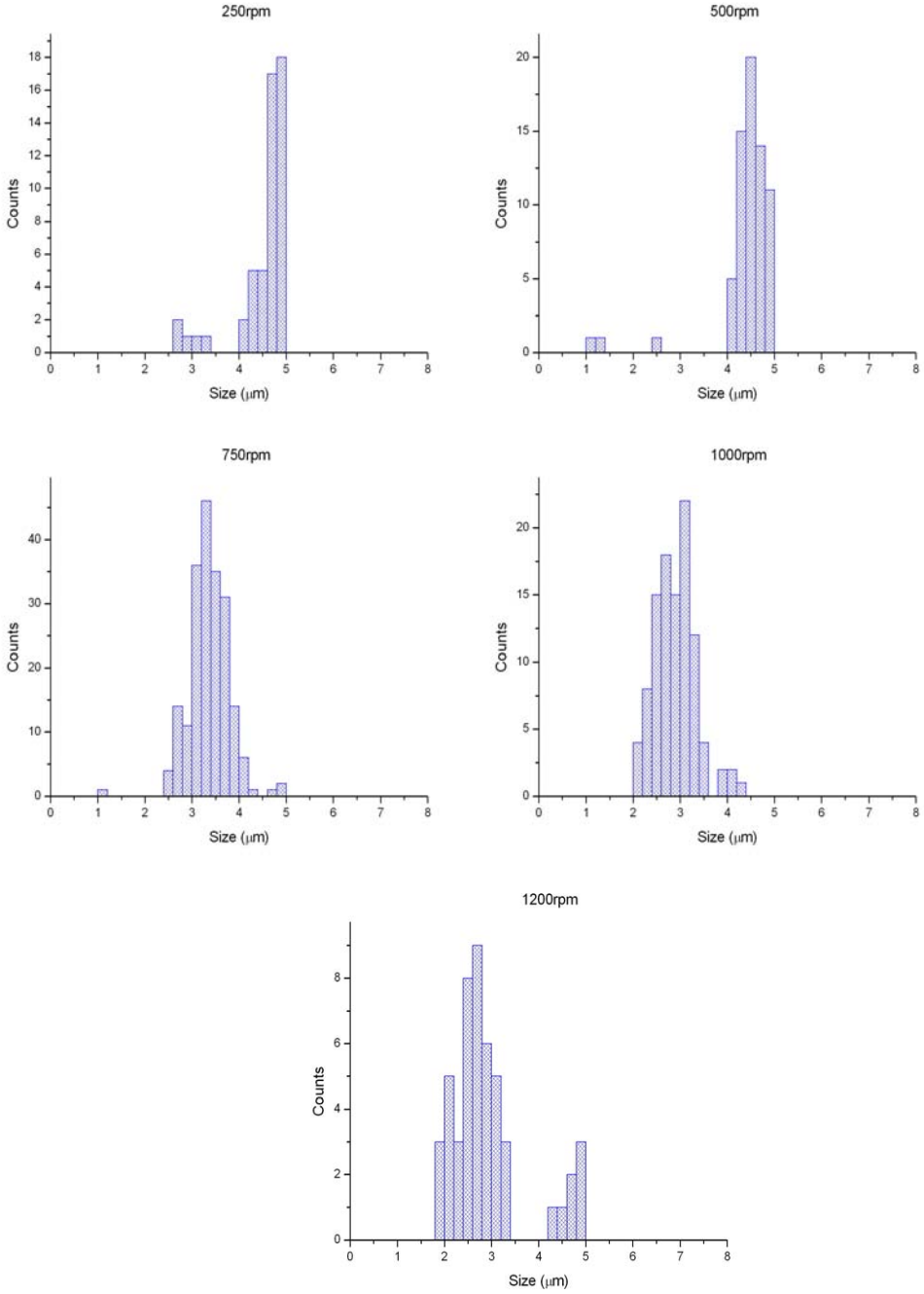

Experiment 3: Rotation speed

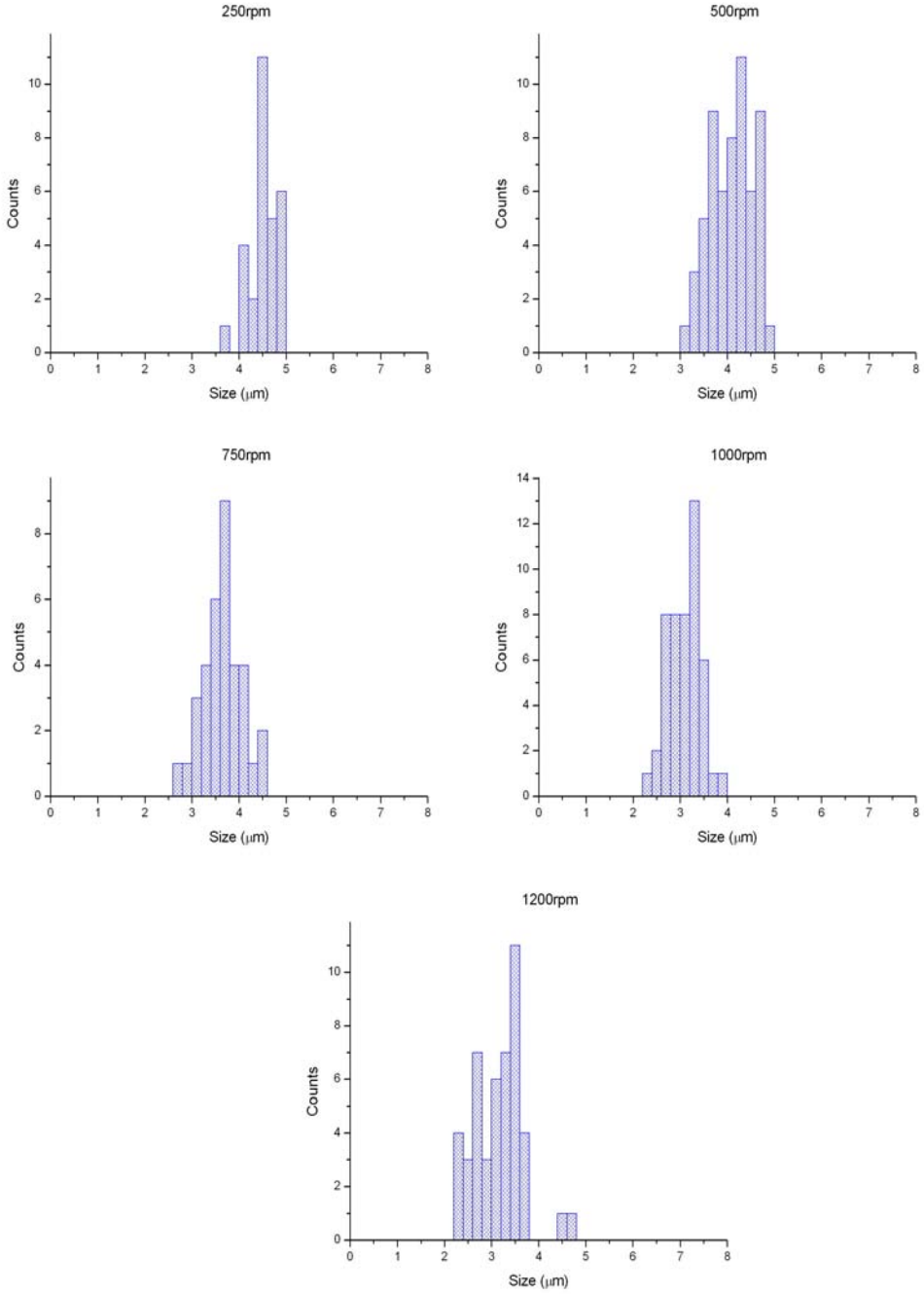

Experiment 4: Rotation speed

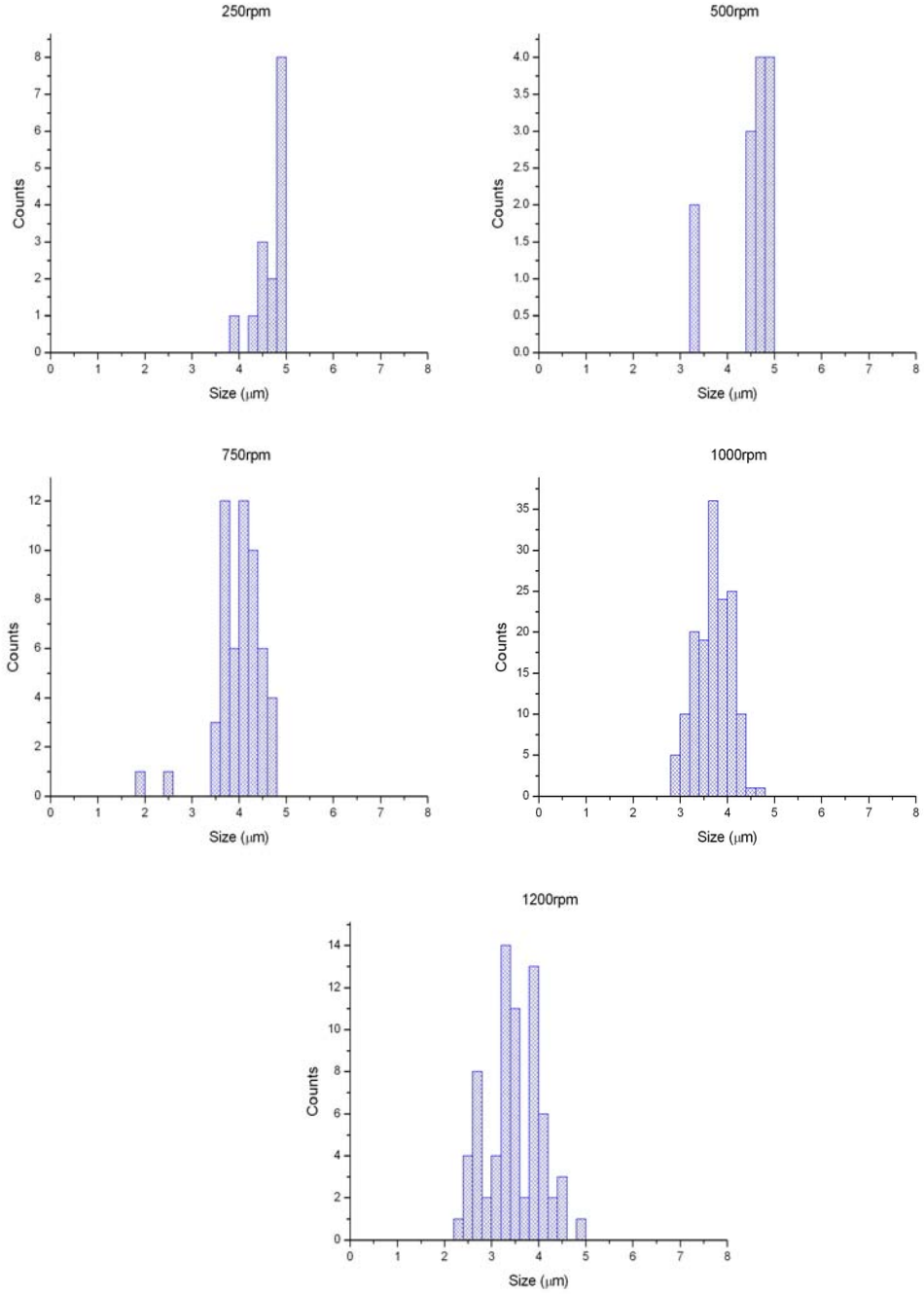

Experiment 5: Rotation speed

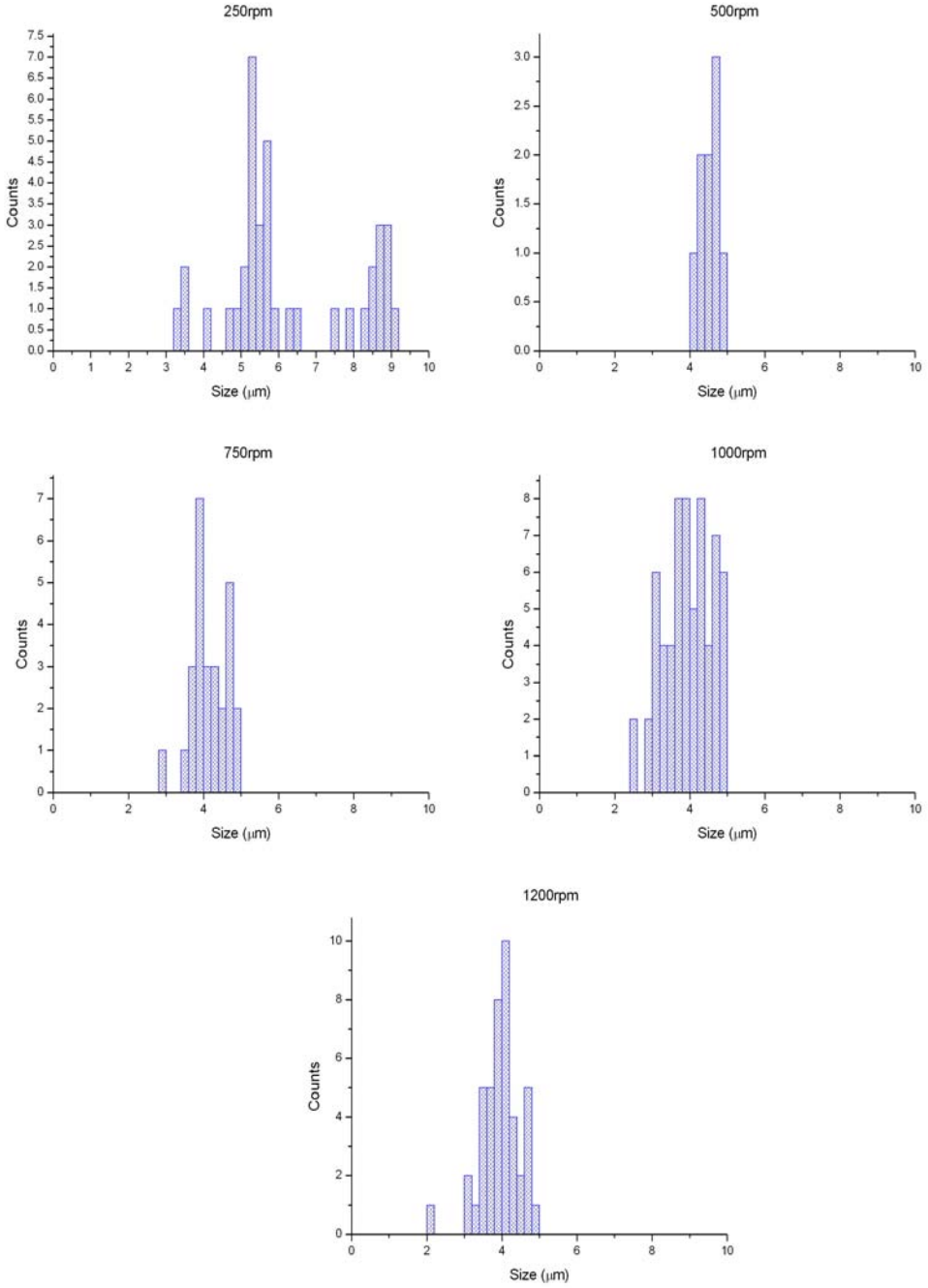

Erklärung

Hiermit erkläre ich, dass ich meine Bachelorarbeit mit dem Thema:

.....

Optimization of Polyelectrolyte Multilayer Capsules

.....

selbständig verfasst sowie alle wesentlichen Quellen und Hilfsmittel angegeben habe.

Name, Vorname: Stalmann, Gertrud Susanne Dorothea

....

Ort, Datum Unterschrift

[Einverständniserklärung für die Nutzung von **Magistra**-/**Magister-, Bachelor-, Master- bzw**. **Diplomarbeiten** in Bibliotheken. Bitte als letzte Seite in die Arbeit einbinden.]

Einverständniserklärung

Ich erkläre mich damit einverstanden, dass die vorliegende Arbeit

Optimization of Polyelectrolyte Multilayer Capsules

in Bibliotheken allgemein zugänglich gemacht wird. Dazu gehört, dass sie

- von der Bibliothek der Einrichtung, in der ich meine Arbeit angefertigt habe, zur Benutzung in ihren Räumen bereit gehalten wird,
- in konventionellen und maschinenlesbaren Katalogen, Verzeichnissen und Datenbanken verzeichnet wird,
- der UB für die lokale Benutzung und für Fernleihzwecke zur Verfügung steht,
- im Rahmen der urheberrechtlichen Bestimmungen für Kopierzwecke genutzt werden kann.

Marburg,

.....	.....
Unterschrift der Autorin/des Autors	Unterschrift der betreuenden Hochschullehrerin/des betreuenden Hochschullehrers